

# Cross-layer Optimization for Wireless Networks with Deterministic Channel Models

Ziyu Shao\*, Minghua Chen\*, A. Salman Avestimehr<sup>+</sup>, and Shuo-Yen Robert Li\*

\*Department of Information Engineering

The Chinese University of Hong Kong, Shatin, N.T., Hong Kong

Email: {zyshao, minghua, bobli}@ie.cuhk.edu.hk

<sup>+</sup>School of Electrical and Computer Engineering, Cornell University, Ithaca, NY 14853, USA

Email: avestimehr@ece.cornell.edu

**Abstract**—Cross-layer optimization is a key step in wireless network design that coordinates the resources allocated to different layers in order to achieve globally optimal network performance. Existing work on cross-layer optimization for wireless networks often adopts simplistic physical-layer models for wireless channels, such as treating interference as noise or interference avoidance. This crude modeling of physical layer often leads to inefficient utilization of resources. In this paper, we adopt a deterministic channel model proposed in [1], [2], a simple abstraction of the physical layer that effectively captures the effect of channel strength, broadcast and superposition in wireless channels. This model allows us to go beyond “treating interference as noise” and as a consequence are able to achieve higher throughput and utility. Within the Network Utility Maximization (NUM) framework, we study the cross-layer optimization for wireless networks based on this deterministic channel model. First, we extend the well-studied conflict graph model to capture the flow interactions over the deterministic channels and characterize the feasible rate region. Then we study distributed algorithms for general wireless multi-hop networks with both link-centric formulation and node-centric formulation. The convergence of algorithms is proved by applying Lyapunov stability theorem and stochastic approximation method. Further, we show the convergence to the bounded neighborhood of optimal solutions with probability one under constant step size and constant update interval. Our numerical evaluations validate the analytical results and show the advantage of deterministic channel model over simple physical layer models such as treating interference as noise.

## I. INTRODUCTION

Since Kelly’s seminal work [3], the network utility maximization (NUM) framework has attracted significant attentions. In this framework, network protocols are understood as distributed algorithms that maximize aggregate user utility under wired or wireless network resource constraints. This framework not only provides a powerful tool to reverse-engineering existing protocols such as Transmission Control Protocol (TCP), but also allows a systematic design of new protocols [4], *e.g.*, cross-layer optimization for resource allocation of wireless networks.

Cross-layer optimization is becoming increasingly important for improving the performance of multi-hop wireless networks such as throughput or utility. Therefore, it has been studied extensively in recently years [4], [5]. However, almost all existing work base on a simple physical layer assumption: treating interference as noise. This incurs a large

gap between the resulted feasible rate region at link layer and the information-theoretic capacity region, which further incurs a large gap between the resulted network performance and the optimal network performance. The information-theoretic capacity region is the largest achievable rate region that interfering wireless information flows can achieve. Thus by cross-layer optimization over the information-theoretic capacity region, if we can fully utilize this capacity region, then we can achieve the highest throughput or utility.

Therefore, in this paper, within the NUM framework, we study the problem of cross-layer optimization over the information-theoretic capacity region of wireless networks. There has been some work on cross-layer optimization for special wireless networks [6]–[8] where their information-theoretic capacity region are known. However, for general wireless network information flow, applying NUM framework to study the cross-layer optimization over the information-theoretic capacity region is very hard mainly because of two reasons.

One reason is the difficulty of characterizing the information-theoretic capacity region of wireless networks in general. In fact, the capacity of most basic networks, such as the relay channel or the interference channel [9], with only three or four nodes has been an open problem for 40 years. The main barrier is the complexity of the flow interaction in wireless channels in addition to the noise in the channel. Therefore, existing studies on wireless NUM [4], [10], [11] mainly base on a simple physical layer assumption: treating interference as noise. However, it is known that “treating interference as noise” is sub-optimal in general and higher rates can be achieved by using more advanced physical layer coding techniques, such as superposition coding [9], successive interference cancellation [9] and interference alignment [12]. To utilize these techniques, we need new abstractions of the physical layer of wireless networks.

The other reason is that even if the exact information-theoretic capacity region is known, distributed optimal scheduling on this capacity region is still a challenging problem. Though Maximum Weight Scheduling (MWS) algorithm proposed in the seminal work [13] is shown to be throughput-optimal, it has the exponential computational complexity [5] even in a centralized manner, *i.e.*, it is NP-complete. Further, the MWS is not amenable to distributed implementation. Then

low-complexity alternatives [5] of MWS are proposed including randomization, maximal scheduling, and random access with message passing. However, in general, they achieve only a small fraction of maximum throughput region or maximum utility [14]–[16].

To address these difficulties, first, we adopt the deterministic channel model of [1], [2], [17], which provides a more accurate, yet simple, abstraction of the physical layer that can be utilized for the cross-layer protocol design. This model allows more flexibility to handle the interference rather than treating it as noise. Second, we adopt Markov approximation framework [18], which enable us to design distributed scheduling algorithms with provable optimality of network performance. Our algorithm design is motivated by a certain (approximate) product-form distribution that can be characterized as the stationary distribution of a simple and distributed Markovian dynamics (time-reversible Markov chain) over the space of schedules (independent sets of conflict graph).

#### A. Summary of Results and Contributions

In this paper, we focus on solving the wireless NUM problem with deterministic channel model in a distributed manner. In other words, we design distributed flow-control and scheduling algorithms to maximize aggregate user utilities under resource constraints of wireless networks with deterministic channel model, *i.e.*, cross-layer optimization over deterministic-channel-model based rate region. The key results and contributions are listed as follows:

- **Characterization of the feasible rate region by extended conflict graph model:** Existing conflict-graph model [5], [19] is based on simple physical-layer assumptions, such as treating interference as noise or modeling interference as erasure. We propose an extended conflict-graph model to capture the effect interference more accurately by using the deterministic channel models [2]. Although in general we can only obtain a subset of the information theoretical capacity region by using this method, for an important special case of multiple-access channels, the extended conflict graph rate region is the same as the capacity region.
- **Distributed solutions for NUM over general wireless multi-hop networks with deterministic channel models:** We consider wireless networks with both link-centric formulation and node-centric formulation [5], where the capacity constraints are stated as balance equations for each link and each node respectively. By applying Markov approximation framework [18] and standard Lagrange dual decomposition method, we construct distributed algorithms to approximately solve the cross-layer optimization problem within the NUM framework.
- **Convergence of the primal-dual flow control algorithm with or without time-scale separation assumption:** Existing work [20]–[22] focuses on the dual algorithm and prove its convergence. In this paper, we focus on the primal-dual algorithm because it has a smoother trajectory than that of the dual algorithm. With the time-scale separation assumption that Markov chain converges

to its stationary distribution instantaneously, the proposed primal-dual algorithm is shown to converge to the optimal solutions globally asymptotically. Without such time-scale separation assumption, the resulted stochastic primal-dual algorithm is shown to converge to a bounded neighborhood of the same optimal solutions with probability one under constant step sizes and constant update intervals.

#### B. Related Work

**Characterization of Capacity Region.** In general, characterizing the capacity region of wireless networks is one of the key open problems in information theory. As a result, in the field of cross-layer optimization and network utility maximization [4], [5], a common approach is to study the conflict-graph-model based feasible rate region [4], [19], [23]–[25], a subset of the exact capacity region. In this approach, interference is treated as noise, and the conflict graph model [5], [19] is used to model the conflicts of interfering wireless links. With this conflict graph model, we know which groups of links can be active simultaneously. Then the feasible rate region is the convex hull of the corresponding rate vectors of independent sets of the conflict graph, where the convex-hull operation is due to a standard time-averaging argument [4], [5].

On the other hand, in the field of information theory, there has been recent efforts to seek approximate capacity region with a guarantee on the gap to the exact region [2], [26]–[29]. In particular, there has been a new deterministic channel model proposed [1], [2], [17], allowing to approximate the information theoretic capacity of various types of wireless networks within a constant number of bits [2], [27]–[30]. This model quantizes the transmitted signal into different signal strength levels and represents the noise by a deterministic cut-off threshold rather than a random variable. Consequently, the bits received below the noise threshold are discarded by the receiver. This deterministic channel model simplifies the wireless flow interaction by eliminating the noise and allows studies to focus on interferences among transmissions.

**Distributed Scheduling.** Independently, distributed optimal scheduling over the capacity region is still a challenging problem [5], [13] even if the exact capacity region is known. A class of distributed imperfect scheduling algorithms are proposed [5], [14], including Maximal Scheduling [14]–[16], [31] and Greedy Maximal Scheduling (GMS) [32]–[35]. Maximal scheduling can only achieve a small fraction of the capacity region [14], [16], [31]. In contrast, Greedy Maximal Scheduling, also known as Longest-Queue-First (LQF) Scheduling, can achieve the whole capacity region if the so-called local-pooling condition is satisfied [32]. However, in general, GMS may only achieve a fraction of the capacity region [33]–[35]. Further, though maximal scheduling and greedy maximal scheduling have low complexity of computation, the overhead for implementation of these imperfect scheduling algorithms in a decentralized manner can increase with the size of the network [5], [14], [33].

Another class of distributed scheduling algorithms are CSMA (Carrier Sense Multiple Access) type random access

algorithms. Recently, a throughput-optimal adaptive CSMA based distributed scheduling algorithm is proposed in [20], and the design has been further explored in [21], [22], [36]–[38]. Inspired by this series of work, we propose in [18] a Markov approximation framework for synthesizing distributed algorithms for general combinatorial network optimization problems, including the Maximum Weight Scheduling problem as a special case. We show that [18] when using the log-sum-exp function to approximate the optimal value of any combinatorial problem, we end up with a solution that can be interpreted as the stationary probability distribution of a class of time-reversible Markov chains. Certain carefully designed Markov chains among this class yield distributed algorithms that solve the log-sum-exp approximated combinatorial network optimization problem.

### C. Outline of the Paper

The remainder of this paper is organized as follows. In Section II, we introduce the system model and the problem formulation. In Section III and Section IV, we propose distributed solutions for general multi-hop wireless networks with link-centric formulation and node-centric formulation respectively. Numerical results are provided in Section V, and conclusions are drawn in Section VI.

## II. SYSTEM MODEL AND PROBLEM FORMULATION

We consider a wireless network with a set of users (source-destination pairs), denoted as  $S$ . Each user  $s \in S$  is associated with a sending rate  $x_s$ , as well as a utility function  $U_s(x_s)$  that measures both the efficiency and fairness of resource allocation algorithms. One commonly used example of utility function is the  $\alpha$ -fairness utility function [39], defined in the following:

$$U^\alpha(x) = \begin{cases} \frac{x^{1-\alpha}}{1-\alpha} & \text{if } \alpha \neq 1 \\ \log x & \text{Otherwise,} \end{cases}$$

where  $\alpha = 1$  corresponds to proportional fairness and  $\alpha \rightarrow \infty$  corresponds to max-min fairness.

We emphasize here that our results apply for *general utility functions* as long as they are twice differentiable, increasing and strictly concave [4], including  $\alpha$ -fairness utility function as a special case.

The utility maximization problem is as follows

$$\begin{aligned} \mathbf{P1:} \quad & \max_{\mathbf{x} \geq 0} \sum_{s \in S} U_s(x_s) \\ \text{s.t.} \quad & \mathbf{x} \in \{\text{feasible rate region}\}. \end{aligned} \quad (1)$$

where  $\mathbf{x}$  is the vector of user's rate (we use bold symbols to denote vectors through the whole paper) and the feasible rate region is a function of information transmission constraints. In general, there are two different ways of stating the feasible rate region: *link-centric formulation* and *node-centric formulation* [5]. In link-centric formulation, the capacity constraints are stated as balance equations for each link and the routes for each user are predetermined. While in node-centric formulation, the capacity constraints are stated as balance equations of incoming rates and outgoing rates for each node.

### A. Deterministic Channel Model

In this paper, we study the problem **P1** over the feasible rate region based on the deterministic channel model of [2]. We first give an intuitive illustration of this model and explain how it captures the effects of channel strength, broadcast, and superposition in wireless networks.

Consider a point-to-point Gaussian channel with a signal-to-noise ratio denoted by SNR, shown in Fig. 1 (a). Consider the binary-expansion of the real-valued input of the Gaussian channel:

$$x = 0.b_1b_2b_3b_4b_5 \dots$$

Intuitively speaking, this sequence of bits goes through the channel and some of them are received above the receiver's noise level and some are received below. One way to capture the effect of noise deterministically is by truncating all bits that are received below noise level. Therefore, we can think of a transmitted signal 'x' as a sequence of bits at different "signal levels," with the highest signal level in 'x' being the most significant bit (MSB) and the lowest level being the least significant bit (LSB). In the deterministic channel model, shown in Fig. 1 (b), the receiver only gets the ' $\rho$ ' most significant bits of 'x'. The correspondence between the number of bits received in the deterministic channel, ' $\rho$ ', and the SNR in the complex Gaussian channel is  $\rho \leftrightarrow \lceil \log \text{SNR} \rceil^+$ . We refer to the parallel links in Fig. 1 (b) as sub-links corresponding to the channel between the transmitter and the receiver.

Next, consider the Gaussian multiple access channel, shown in Fig. 2 (a). The deterministic model for this channel is constructed similarly to the point-to-point channel (Fig. 2 (b)), with  $\rho_1$  and  $\rho_2$  bits received above the noise level from users 1 and 2, respectively. To model the superposition of signals at the receiver, the bits received on each level are added modulo two. Addition modulo two, rather than normal integer addition, is chosen to make the model more tractable. As a result, the levels do not interact with one another. This way of modeling interaction is in some sense similar to the collision model. In the collision model, if two packets arrive simultaneously at a receiver, both are dropped; similarly, here, if two bits arrive simultaneously at the same signal level, the receiver gets only their modulo two sum, which means it cannot figure out any of them. However, in this case, the most significant bits of the stronger user remain intact, contrary to the simplistic collision model in which the entire packet is lost when there is collision. This is reminiscent of the familiar capture phenomenon in CDMA systems, *i.e.*, the strongest user can be heard even during simultaneous transmissions by multiple users.

Based on the intuition obtained so far, it is straightforward to think of a deterministic model for the broadcast scenario. Consider a single source broadcasting to two receivers shown in Fig. 2 (c). Fig. 2 (d) shows the deterministic model for the Gaussian broadcast channel (BC). The user with the stronger channel observes  $\rho_1$  significant bits from the input. The user with the weaker channel observes only  $\rho_2$  of the most significant bits ( $\rho_2 < \rho_1$ ).

We now bring a formal definition of the deterministic channel model.

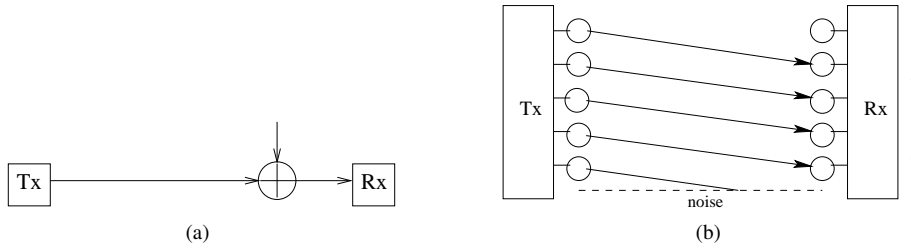


Fig. 1. (a) Gaussian model and (b) deterministic model for point-to-point channel.

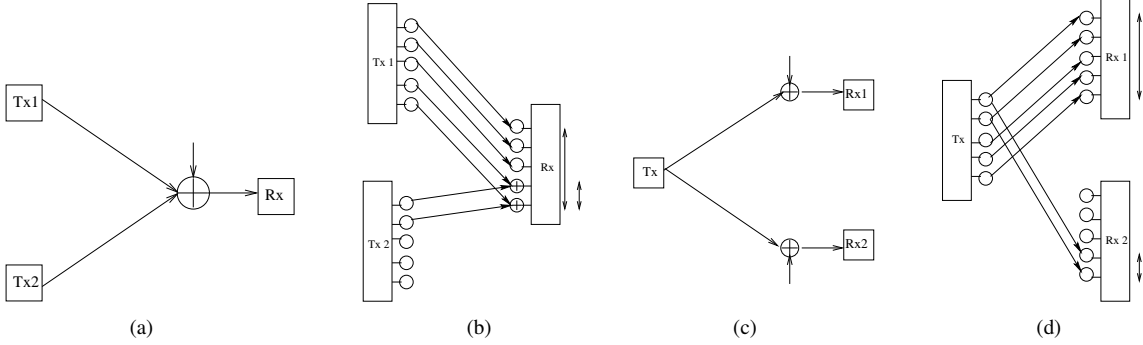


Fig. 2. Gaussian (a) and deterministic (b) models for MAC. Gaussian (c) and deterministic (d) models for BC.

**Definition 1. (Definition of the deterministic model [1], [2])**

Consider a wireless network consisting of a set of nodes  $V$  and a set of channels, where  $K = |V|$  is the number of nodes. Communication from node  $i$  to node  $j$  has a non-negative integer gain  $\rho_{(i,j)}$  associated with it. At each time  $t$ , node  $i$  transmits a vector  $\mathbf{x}_i[t] \in \mathbb{F}_2^\omega$  and receives a vector  $\mathbf{y}_i[t] \in \mathbb{F}_2^\omega$  where  $\omega = \max_{i,j}(\rho_{(i,j)})$ . The received signal at each node is a deterministic function of the transmitted signals at the other nodes, with the following input-output relation: if the nodes in the network transmit  $\mathbf{x}_1[t], \mathbf{x}_2[t], \dots, \mathbf{x}_K[t]$  then the received signal at node  $j$ ,  $1 \leq j \leq K$  is:  $\mathbf{y}_j[t] = \sum_{k=1}^K \mathbf{W}^{\omega - \rho_{k,j}} \mathbf{x}_k[t]$  for all  $1 \leq k \leq V$ , where  $\mathbf{W}$  is the  $\omega \times \omega$  shift matrix and the summation and multiplication is in  $\mathbb{F}_2$ .

**B. Conflict Graph Based Model**

The deterministic channel model based wireless network is represented as a graph  $G=(V, L)$ , where  $V$  is the set of nodes and  $L$  is the set of links(channels) between nodes. Each link(channel)  $(i, j) \subset L$  consists of  $\rho_{(i,j)}$  sub-links (each with one-unit capacity), where  $i, j \in V$  and  $\rho_{(i,j)}$  is the channel gain from node  $i$  to node  $j$ . In this paper, we cast the consecutive signal level constraint to make the model tractable. This means that for the channel  $l$  with the channel gain  $\rho_l$ , the transmitter can only transmit over one of the  $\frac{\rho_l(\rho_l+1)}{2}$  configurations of channel  $l$  that correspond to all possible combinations of consecutive sub-links within the channel  $l$ . For example, in Fig. 3 (a), for channel  $AR$  with channel gain  $\rho_{AR} = 2$  and two sublinks  $a_1, a_2$ , there are 3 configurations:  $\{a_1\}$ ,  $\{a_1, a_2\}$ , and  $\{a_2\}$ .

To characterize the feasible rate region of wireless network  $G$ , we need to model the interferences of deterministic channels first. Note that deterministic channel model deals with the interference in the sub-link level, a fine granularity of

interference. Therefore, we need to model the conflicts of sublinks belonging to different channels. At a first glance, we can apply the existing conflict graph model [5], [19], where each vertex in conflict graph corresponds to a sublink in  $G$  and each edge in conflict graph corresponds to a conflict between two sublinks in  $G$ . However, this conflict graph model fails to capture the conflicts of sublinks because it does not account for the consecutive signal level constraint. It also takes much effort to modify this conflict graph model to accommodate the constraint. More disadvantages of this sublink-based conflict graph model are discussed in the next subsection. Therefore, we propose the following *extended conflict graph model*.

**Definition 2.** The conflict graph  $G_c$  of a graph  $G$  is an undirected graph  $G_c = (V_c, A)$ .  $V_c$  is the set of vertices, where each vertex represents one link configuration in  $G$ .  $A$  is the set of connections of adjacent vertices, where each connection represents conflict of two configurations. Two vertices are adjacent if for the corresponding two configurations, either they belong to the same set of configurations for one channel(link) or there exist two sub-links within two configurations, one for each, conflicting with each other, i.e., intersecting at the same signal level of one node.

Note that all possible configurations for the same channel are conflict with others, since given any one channel, only one configuration for this channel can be activated at a time. Then we introduce the definition of independent set, shown as follows:

**Definition 3.** An independent set of the conflict graph  $G_c = (V_c, A)$  is a subset  $M \subset V_c$  of vertices that no two of which are adjacent (i.e.,  $(s, t) \notin A$  for all  $s, t \in M$ ), i.e., the set of channel (link) configurations that can be activated simultaneously.

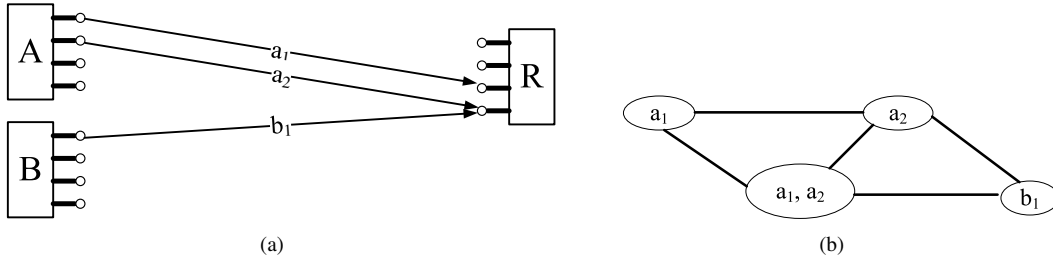


Fig. 3. An example of deterministic wireless network with channel gains  $\rho_{AR} = 2$  and  $\rho_{BR} = 1$  (a) and its corresponding conflict graph (b). All independent sets are:  $\emptyset$ ,  $\{a_1\}$ ,  $\{a_2\}$ ,  $\{b_1\}$ ,  $\{a_1, a_2\}$ , and  $\{\{a_1\}, \{b_1\}\}$ .

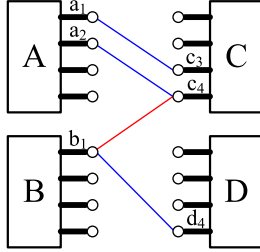


Fig. 4. Example of wireless networks with broadcast advantages. For transmission initiated by  $a_1$ , its receiver is  $c_3$ , for transmission initiated by  $a_2$ , its receiver is  $c_4$ , and for transmission initiated by  $b_1$ , its receivers are  $c_4$  and  $d_4$ . Possible transmissions:  $(a_1, \{c_3\})$ ,  $(a_2, \{c_4\})$ ,  $[(a_1, \{c_3\}), (a_2, \{c_4\})]$ ,  $(b_1, \{c_4\})$ ,  $(b_1, \{d_4\})$  and  $(b_1, \{c_4, d_4\})$ .

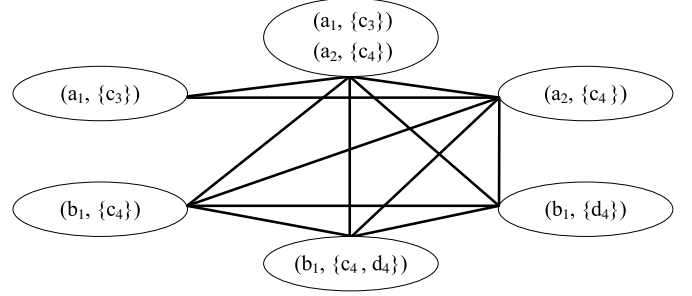


Fig. 5. Corresponding conflict graph for the network shown in Fig. 3. All independent sets are:  $\emptyset$ ,  $\{(a_1, \{c_3\})\}$ ,  $\{(a_2, \{c_4\})\}$ ,  $\{(a_1, \{c_3\}), (a_2, \{c_4\})\}$ ,  $\{(b_1, \{c_4\})\}$ ,  $\{(b_1, \{d_4\})\}$ ,  $\{(b_1, \{c_4, d_4\})\}$ ,  $\{(a_1, \{c_3\}), (b_1, \{c_4\})\}$ ,  $\{(a_1, \{c_3\}), (b_1, \{d_4\})\}$ , and  $\{(a_1, \{c_3\}), (b_1, \{c_4, d_4\})\}$ .

Here we give an example. For the wireless network shown in Fig. 3 (a), the corresponding conflict graph and independent sets are shown in Fig. 3 (b). Note that in Fig. 3 (a), sub-link  $a_2$  conflicts with sub-link  $b_1$ , *i.e.*, intersecting at the same signal level of node  $R$ .

Now we take into account the broadcast advantage of wireless medium, *i.e.*, a single packet transmission might be overheard by a subset of receiver nodes within range of the transmitter. Therefore a one-hop wireless transmission with broadcast advantage can be represented by a hyperlink  $(s, \{R_s\})$ , where  $s$  is the transmitter,  $\{R_s\}$  is the set of receivers, and  $|R_s| \geq 1$ . By modeling wireless networks with broadcast advantages as hypergraphs, we can directly extend the definitions of conflict graph and associated independent set to conflict hypergraph model. When  $|R_s| = 1, \forall s$ , the conflict hypergraph model degenerates into the above conflict graph model. We omit the formal definition of conflict hypergraph here and show an example instead. The scenario is shown in Fig. 4. Corresponding conflict graph and independent sets are shown in Fig. 5. Note that in Fig. 4, when subnode  $b_1$  sends one packet to subnode  $d_4$ , the subnode  $c_4$  overhears this packet. Therefore if at this time subnode  $a_2$  also sends one packet to  $c_4$ , then  $c_4$  receives two corrupted packets, *i.e.*, two simultaneous transmissions  $b_1 \rightarrow d_4$  and  $a_2 \rightarrow c_4$  collide with each other.

### C. Extended Conflict Graph Model vs. Existing Conflict Graph Model.

In this subsection, we further discuss the advantage of using link-configuration based extended conflict graph model over sublink based existing conflict graph model. As stated in

last subsection, there are two ways to use conflict graph to capture link conflicts in the deterministic model. One is the our extended conflict graph model. This model is based on the channel(link) configuration, *i.e.*, all possible combinations of consecutive sub-links within the channel. The other is the existing conflict graph model [5], [19], which is based on sub-links.

First, we discuss the fundamental difference in complexity between these two models. For the constraint of consecutive signal levels, the extended conflict graph model can easily handel it based on channel-configurations, while the existing conflict graph model needs global coordination between nodes. Now we consider a  $k$ -hop flow and suppose each link has  $\rho$  sublinks. By the extended conflict graph model, each link maintains  $\frac{\rho(\rho+1)}{2}$  link configurations, and there are only one  $k$ -hop path based on link configurations. While by the existing conflict graph model, each link maintains  $\rho$  sublinks and there are at least  $\rho^k$   $k$ -hop paths based on sublinks. An example is shown in Fig.6, where a flow transverses from  $A$  to  $E$ ,  $k = 4$  and  $\rho = 3$ .

In general, given a deterministic network with  $\Theta(\rho)$  sublinks per link and  $\Theta(k)$  hops per-flow, by extended conflict graph model, we have  $\Theta(\rho^2)$  sublinks per-link and  $\Theta(1)$  path per-flow; whereas by existing conflict graph model, we have  $\Theta(\rho)$  sublinks per-link and  $\Theta(\rho^k)$  paths per-flow.

Second, we discuss the impacts of running primal, dual, and prima-dual resource allocation algorithms over the underlying conflict graph model. In general, the dual algorithm and the primal-dual algorithm solve the resource allocation problem exactly, whereas the primal algorithm solves it only approximately [40]. Further, given the underlying multipath setting,

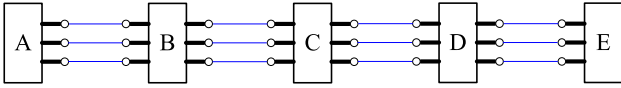


Fig. 6. A deterministic wireless network with four links  $AB$ ,  $BC$ ,  $CD$  and  $DE$ . Each link has three sublinks. There is a flow transverse from  $A$  to  $E$ . By the extended conflict graph model, each link maintains six link configurations and there is only one four-hop path. In contrast, by the existing conflict graph model on sublinks, each link maintains three sublinks and there are at least eighty-one four-hop paths.

the objective functions are not strictly concave. Standard dual gradient algorithms fail to work since the gradient is not everywhere defined [40], [41]. Dual subgradient algorithms are proposed as alternatives. However, the convergence of dual variables in these subgradient algorithms is typically slow. Further, recovering optimal primal variables from optimal dual variables requires solving another optimization problem [40], which may not have distributed solutions. What is more, it is known that multipath setting usually incurs the instability of primal-dual algorithms [41], [42].

Therefore, in this paper, we propose the extended conflict graph model instead of adopting the existing conflict graph model.

#### D. Feasible Rate Region

The feasibility of simultaneous transmissions can be captured by the extended conflict graph for wireless networks with deterministic channel model. As a result, the feasible rate region is characterized as a convex hull of the feasible rates supported by possible independent sets on this extended conflict graph [19].

For some important cases such as single-hop multiple-access wireless networks, we show that the conflict graph based rate region is equal to the information-theoretic capacity region. Details can be found at Appendix-A.

For general wireless networks, the conflict graph based rate region is only a subset of the information-theoretic capacity region. One example is shown in Fig. 7 [27]. We can show that the rate tuple  $(3,2)$  is out of the conflict graph based rate region, since in our conflict graph model, two bits arrive simultaneously at the same signal levels of the receiver are dropped.

The characterization of the information-theoretic capacity region of general wireless networks is open. Therefore, in this paper, we focus on general deterministic channel and the extended conflict graph based rate region. To save the heavy notation, we focus on the extended conflict graph model. The extension to extended conflict hypergraph model is straightforward.

### III. NUM OVER GENERAL MULTI-HOP NETWORK: LINK-CENTRIC FORMULATION

In this section, we focus on the link-centric formulation based feasible rate region. Consider a multi-hop network  $G=(V, L)$ , where each user is associated with a single path. Let  $H$  be the set of all independent sets over the corresponding conflict graph  $G_c$ . Let  $\mathbf{q} = [q_h, h \in H]^T$  be the vector

of probability (or time fraction) of all independent sets. Let  $\mathbf{x} = [x_s, s \in S]^T$  be the vector of sending rates of users. Let  $\lambda_{l,h}$  be the capacity of link  $l$  within the independent set  $h$ .  $\lambda_{l,h} = 0$  means link  $l$  is not activated within the independent set  $h$ . We also let  $\{s : l \in s\}$  denote the set of users sharing the link  $l$ .

Consider the following master utility maximization problem over  $G_c$ .

$$\begin{aligned} \text{MP} : \quad & \max_{\mathbf{x} \geq 0, \mathbf{q} \geq 0} \sum_{s \in S} U_s(x_s) & (2) \\ \text{s.t.} \quad & \sum_{s: l \in s} x_s \leq \sum_{h \in H} \lambda_{l,h} q_h, \quad \forall l \in L & (3) \\ & \sum_{h \in H} q_h = 1. \end{aligned}$$

Solving the master problem **MP** (2) is very challenging because the scheduling subproblem is NP-hard in general. To see that, first, by relaxing the first set of inequality constraints (3) in problem **MP**, we get its partial Lagrangian:

$$L(\mathbf{x}, \mathbf{q}, \mathbf{r}) = \sum_{s \in S} U_s(x_s) - \sum_{l \in L} r_l \left( \sum_{s: l \in s} x_s - \sum_{h \in H} \lambda_{l,h} q_h \right),$$

where  $\mathbf{r} = [r_l, l \in L]^T$  is the vector of Lagrange multipliers. Note that

$$\begin{aligned} \sum_{l \in L} r_l \sum_{s: l \in s} x_s &= \sum_{s \in S} x_s \sum_{l: l \in s} r_l, \\ \sum_{l \in L} r_l \sum_{h \in H} \lambda_{l,h} q_h &= \sum_{h \in H} q_h \sum_{l \in L} \lambda_{l,h} r_l. \end{aligned}$$

Since the Slater constraint qualification conditions hold for convex optimization problems with concave objective functions and linear constraints [43], the strong duality holds for problem **MP**. Thus the problem **MP** can be solved by finding the saddle points of  $L(\mathbf{x}, \mathbf{q}, \mathbf{r})$  via solving the following problem:

$$\begin{aligned} \text{DP} : \quad & \min_{\mathbf{r} \geq 0} \left( \max_{\mathbf{x} \geq 0} \left( \sum_{s \in S} U_s(x_s) - \sum_{s \in S} x_s \sum_{l: l \in s} r_l \right) \right. \\ & \left. + \max_{\mathbf{q} \geq 0} \left( \sum_{h \in H} q_h \sum_{l \in L} \lambda_{l,h} r_l \right) \right) & (4) \\ \text{s.t.} \quad & \sum_{h \in H} q_h = 1. \end{aligned}$$

The above problem can be solved successively in  $\mathbf{q}, \mathbf{x}, \mathbf{r}$ . The key challenge lies in solving the sub-problem in  $\mathbf{q}$ , which is the Maximum Weighted Independent Set (MWIS) problem [44]:

$$\begin{aligned} \text{MWIS} : \quad & \max_{\mathbf{q} \geq 0} \sum_{h \in H} q_h \sum_{l \in L} \lambda_{l,h} r_l & (5) \\ \text{s.t.} \quad & \sum_{h \in H} q_h = 1. \end{aligned}$$

It is not hard to see that the optimal value of the **MWIS** problem is given by computing the max function:  $\max_{h \in H} \sum_{l \in L} \lambda_{l,h} r_l$ . Denote

$$H^* = \arg \max_{h \in H} \sum_{l \in L} \lambda_{l,h} r_l & (6)$$

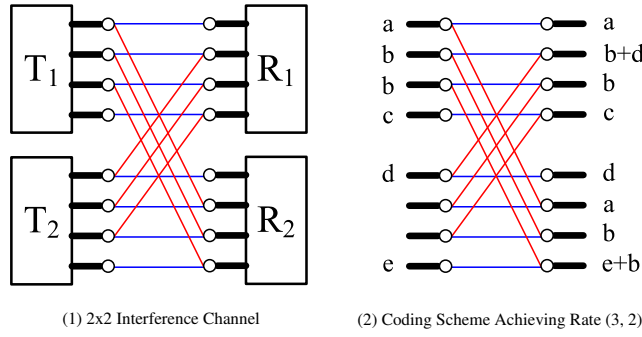


Fig. 7. [27]. Subfig (1) shows a 2x2 deterministic interference channel with channel gains  $\rho_{T_1 R_1} = \rho_{T_2 R_2} = 4$  and  $\rho_{T_1 R_2} = \rho_{T_2 R_1} = 3$ . Subfig (2) shows a coding scheme achieving the rate tuple (3,2), where  $T_1$  sends  $a, b, b, c$  to  $R_1$  and  $T_2$  sends  $d, \emptyset, \emptyset, e$  to  $R_2$ .  $R_1$  can decode and obtain  $a, b, c$ , while  $R_2$  can decode and obtain  $d, e$ .

as the set of maximum weighted independent set. When there are multiple maximum weighted independent sets, i.e.,  $|H^*| > 1$ , one set is picked uniformly among  $H^*$ . Then optimal distribution for MWIS problem is  $q_h = \frac{1}{|H^*|}, \forall h \in H^*; q_h = 0, \forall h \in H - H^*$ .

#### A. Markov Approximation

The MWIS problem is NP-hard [44] and hard to approximate even in a centralized manner [44]. Here we apply the Markov approximation framework [18] to solve the problem in a distributed way. There are two steps of Markov approximation framework [18]: log-sum-exp approximation and distributed construction of Markov chain.

First, we apply the log-sum-exp approximation

$$\max_{h \in H} \sum_{l \in L} \lambda_{l,h} r_l \approx \frac{1}{\beta} \log \left[ \sum_{h \in H} \exp \left( \beta \sum_{l \in L} \lambda_{l,h} r_l \right) \right], \quad (7)$$

where  $\beta$  is a positive constant.

Let  $|H|$  denote the size of the set  $H$ , then the approximation accuracy is known as follows:

#### Proposition 1.

$$\begin{aligned} \max_{h \in H} \sum_{l \in L} \lambda_{l,h} r_l &\leq \frac{1}{\beta} \log \left[ \sum_{h \in H} \exp \left( \beta \sum_{l \in L} \lambda_{l,h} r_l \right) \right] \\ &\leq \max_{h \in H} \sum_{l \in L} \lambda_{l,h} r_l + \frac{1}{\beta} \log |H| \end{aligned} \quad (8)$$

*Proof:* Given  $\beta > 0$ , let

$$\phi(h) \triangleq \sum_{l \in L} \lambda_{l,h} r_l, \forall h \in H,$$

we have

$$\exp(\max_{h \in H} \beta \phi(h)) \leq \sum_{h \in H} \exp[\beta \phi(h)] \leq |H| \exp(\max_{h \in H} \beta \phi(h)).$$

Then

$$\max_{h \in H} \beta \phi(h) \leq \log \left( \sum_{h \in H} \exp[\beta \phi(h)] \right) \leq \max_{h \in H} \beta \phi(h) + \log |H|$$

By dividing  $\beta$  in both sides, we obtain the inequality (8). ■

Now we have some important observations shown in the following proposition.

**Proposition 2.**  $\frac{1}{\beta} \log \left[ \sum_{h \in H} \exp \left( \beta \sum_{l \in L} \lambda_{l,h} r_l \right) \right]$  is the optimal value of the following optimization problem

$$\begin{aligned} \text{MWIS} - \beta : \max_{q \geq 0} & - \frac{1}{\beta} \sum_{h \in H} q_h \log q_h + \sum_{h \in H} q_h \sum_{l \in L} \lambda_{l,h} r_l \\ \text{s.t.} & \sum_{h \in H} q_h = 1. \end{aligned} \quad (9)$$

and the corresponding unique optimal solution is

$$q_h(\beta \mathbf{r}) = \frac{\exp \left( \beta \sum_{l \in L} \lambda_{l,h} r_l \right)}{\sum_{h \in H} \exp \left( \beta \sum_{l \in L} \lambda_{l,h} r_l \right)}, \forall h \in H. \quad (10)$$

*Proof:* By solving equations of KKT(Karush-Kuhn-Tucker) condition [43] for problem (9), we obtain the desired results. ■

From (10), we can see that  $q_h(\beta \mathbf{r})$ , the probability for independent set  $h$ , is proportional to its weight  $\sum_{l \in L} \lambda_{l,h} r_l$ . Therefore, maximum weighted independent sets  $H^*$  (6) still get the highest probability to be scheduled.

By time-sharing among different independent sets  $h$  according to their portions  $q_h(\beta \mathbf{r})$ , we can solve the problem MWIS  $-\beta$ , and hence the problem MWIS, approximately. Therefore, by the log-sum-exp approximation in (7), we are implicitly solving an approximated version of the problem MWIS, off by an entropy term  $-\frac{1}{\beta} \sum_{h \in H} q_h \log q_h$ .

Second, the  $q_h(\beta \mathbf{r}), h \in H$  in (10) can be interpreted as the stationary distribution of a time reversible Markov chain, whose states are the independent sets in  $H$ . Therefore, the second step of Markov approximation framework is to design and implement such a Markov chain in a distributed manner.

#### B. Design and Implementation of Markov Chain

To construct a time-reversible Markov chain with its stationary distribution  $q_h(\beta \mathbf{r}), h \in H$  in (10), we let  $h \in H$  be the state of the Markov chain. Denote  $h, h' \in H$  as any two states of Markov chain, and denote  $q_{h,h'}$  as the non-negative transition rate from state  $h$  to  $h'$ . It is sufficient to design  $q_{h,h'}$  so that [45]

- the resulting Markov chain is irreducible, i.e., any two states are reachable from each other, either directly or via other states.

- the detailed balance equation is satisfied: for all  $h$  and  $h'$  in  $H$  and  $h \neq h'$ ,  $q_h(\beta \mathbf{r}) q_{h,h'} = q_{h'}(\beta \mathbf{r}) q_{h,h}$ .

Let link configuration  $l_k$  denote the link  $l$  under its configuration  $k$ , and  $\lambda_{l_k,h}$  denote the capacity of link configuration  $l_k$  within independent set  $h$ . Recall that for link(channel)  $l$  with channel gain  $\rho_l$ , there are  $\frac{\rho_l(\rho_l+1)}{2}$  configurations of link(channel)  $l$ .

We start by only allowing direct transitions between two “adjacent” states (independent sets)  $h$  and  $h'$  that differ by one and only one link configuration. Note that doing so will not affect the stationary distribution for time-reversible Markov chains [18, Section II]. Then by this design, the transition from  $h'$  to  $h = h' \cup \{l_k\}$  corresponds to link configuration  $l_k$  starting its transmission. Similarly, the transition from  $h$  to  $h'$  corresponds to link configuration  $l_k$  finishing its on-going transmission.

Now, consider two states  $h$  and  $h'$  where  $h = h' \cup \{l_k\}$ . We set  $q_{h,h'}$  to  $\lambda_{l_k,h}$ , and

$$\begin{aligned} q_{h',h} &= \lambda_{l_k,h} \exp(\beta(\sum_{l \in h} \lambda_{l,h} r_l - \sum_{l \in h'} \lambda_{l,h'} r_l)) \\ &= \lambda_{l_k,h} \exp(\beta \lambda_{l_k,h} r_l). \end{aligned}$$

To achieve transition rate  $q_{h',h}$ , the transmitter of link  $l$  sets a timer  $T_{l,k}$  for link configuration  $l_k$ , which counts down according to an exponential distribution with rate  $\lambda_{l_k,h} \exp(\beta \lambda_{l_k,h} r_l)$ . When the timer  $T_{l,k}$  expires, link  $l$  starts to transmit under the configuration  $k$ . During the countdown process, if the transmitter of link  $l$  determines that another interfering link configuration is in transmission, link configuration  $l_k$  will freeze its count-down process. This could be done in various ways, for instance by the receiver of link  $l$  communicating busy/idle notification to the transmitter using a dedicated low-rate feedback channel.

When the transmission of interfering link is over, timer  $T_{l,k}$  counts down according to the residual back-off time, which is still exponential distributed with the same rate, because of the memoryless property of exponential distributions.

The transition rate  $q_{h,h'}$  can be achieved by the transmitter of link  $l$  under configuration  $k$  setting its transmission time to follow an exponential distribution with rate  $\lambda_{l_k,h}$ .

The corresponding pseudocode is shown in Algorithm 1. Then we establish the following result:

**Proposition 3.** *Algorithm 1 in fact implements a time-reversible Markov chain with stationary distribution in (10).*

The proof is relegated to Appendix-B

### C. Solving the Approximated Problem by the Primal-Dual Algorithm

By the log-sum-exp approximation, it is not hard to see that we are actually solving a problem close to the original problem **MP**:

$$\begin{aligned} \mathbf{MP} - \beta : \max_{\mathbf{x} \geq 0, \mathbf{q} \geq 0} \quad & \sum_{s \in S} U_s(x_s) - \frac{1}{\beta} \sum_{h \in H} q_h \log q_h \quad (11) \\ \text{s.t.} \quad & \sum_{s: l \in s} x_s \leq \sum_{h \in H} \lambda_{l,h} q_h, \quad \forall l \in L \\ & \sum_{h \in H} q_h = 1. \end{aligned}$$

---

### Algorithm 1 Implementation of Markov Chain

---

- 1: The following procedure runs on each individual link(channel) independently. We focus on a particular link(channel)  $l$  with the channel gain  $\rho_l$ .
  - 2: **procedure** INITIALIZATION
  - 3:     Obtains  $r_l$  based on queue-length of link(channel)  $l$
  - 4:     index  $\leftarrow 0$
  - 5:     Invoke Procedure Wait-and-Transmit( $l$ )
  - 6: **end procedure**
  - 7: **procedure** WAIT-AND-TRANSMIT( $l$ )
  - 8:     generates  $\frac{\rho_l(\rho_l+1)}{2}$  timers  $T_{l,k}$ ,  $k = 1, 2, \dots, \frac{\rho_l(\rho_l+1)}{2}$  following exponential distributions with rates  $\lambda_{l_k} \exp(\beta \lambda_{l_k} r_l)$  respectively and begin counting down. Each timer  $k$  is associated with link configuration  $l_k$ , a possible configuration of link  $l$ , and  $\lambda_{l_k}$  is the corresponding capacity of link configuration  $l_k$ .
  - 9:     **while** the timer  $T_{l,k^*}$  with  $k^* = \arg \min_k T_{l,k}$  does not expire **do**
  - 10:         **if** there is a transmission of interfering links **then**
  - 11:             index  $\leftarrow 1$
  - 12:             **break**
  - 13:         **end if**
  - 14:     **end while**
  - 15:     Terminates all current countdown processes
  - 16:     **if** index = 1 **then**
  - 17:         index  $\leftarrow 0$
  - 18:         Invoke Procedure Wait-and-Transmit( $l$ )
  - 19:     **else**
  - 20:         Sets the transmit time to follow an exponential distribution with rate  $\lambda_{l_{k^*}}$  and transmits
  - 21:     **end if**
  - 22: **end procedure**
- 

Denote the optimal solution of master problem **MP** (2) by  $\mathbf{x}^*$ , and the optimal solution of problem **MP**  $-\beta$  (11) by  $\hat{\mathbf{x}}$ , then we have

$$\left| \sum_{s \in S} (U_s(\hat{x}_s) - U_s(x_s^*)) \right| \leq \frac{\log |H|}{\beta} \quad (12)$$

As  $\beta \rightarrow \infty$ ,  $\hat{\mathbf{x}}$  approaches  $\mathbf{x}^*$ .

**MP**  $-\beta$  is equivalent to the following problem:

$$\begin{aligned} \mathbf{DP} - \beta : \min_{\mathbf{r} \geq 0} \max_{\mathbf{x} \geq 0} \quad & L_\beta(\mathbf{x}, \mathbf{r}) = \sum_{s \in S} (U_s(x_s) - x_s \sum_{l: l \in s} r_l) \\ & + \frac{1}{\beta} \log \left[ \sum_{h \in H} \exp(\beta \sum_{l \in L} \lambda_{l,h} r_l) \right] \quad (13) \end{aligned}$$

The problem **DP**  $-\beta$  (13) can be solved by either a dual algorithm or a primal-dual algorithm. Existing work [20], [21] all focused on dual algorithms. We prefer the primal-dual algorithm because of its fast convergence rate (only one time-scale) and smoothness of changes in parameters.

After denoting the user rates by  $x_s$ ,  $s \in S$  and the link prices by  $r_l$ ,  $l \in L$ , we propose a primal-dual algorithm as

follows:

$$\begin{cases} \dot{x}_s = \alpha_s \left[ U'_s(x_s) - \sum_{l:l \in S} r_l \right]_{x_s}^+ \\ \forall s \in S \text{ user rates updating} \\ \dot{r}_l = k_l \left[ \sum_{s:l \in S} x_s - \sum_{h \in H} \lambda_{l,h} q_h \right]_{r_l}^+ \\ \forall l \in L \text{ link prices updating} \end{cases}, \quad (14)$$

where  $\alpha_s (s \in S)$  and  $k_l (l \in L)$  are positive constants, and function  $[b]_a^+ = \max(0, b)$  if  $a \leq 0$  and equals  $b$  otherwise.

With the time-scale separation assumption that Markov chain converges to its stationary distribution instantaneously compared to the time-scale of adaption of  $\mathbf{x}$  and  $\mathbf{r}$ , we have the following result:

**Theorem 1.** *The primal-dual algorithm (14) is globally asymptotically stable.*

The proof is relegated to Appendix-C

Since the equilibrium point of primal-dual algorithm (14) solves the problem  $\mathbf{DP} - \beta$  (13) exactly, it also solves the problem  $\mathbf{MP} - \beta$  (11) exactly. Therefore, the primal-dual algorithm (14) solves the master problem  $\mathbf{MP}$  (2) approximately in a distributed way.

#### D. Convergence of Stochastic Primal-Dual Algorithm

Note that in (14),  $\sum_{h \in H} \lambda_{l,h} q_h$  is the expectation of rate for link  $l$ , i.e., the ensemble average of rate for link  $l$ . However, it is hard to obtain this ensemble average (expectation) value exactly. In practice, we estimate this ensemble average value with the time average value. Therefore, the above primal-dual algorithm (14) turns to a stochastic primal-dual algorithm, given as follows:

$$\begin{cases} x_s(m+1) = \left[ x_s(m) + \epsilon(m) \left( U'_s(x_s(m)) - \sum_{l:l \in S} r_l(m) \right) \right]_+ \\ \forall s \in S \text{ user rates updating} \\ r_l(m+1) = \left[ r_l(m) - \epsilon(m) (\bar{\theta}_l(m) - \sum_{s:l \in S} x_s(m)) \right]_+ \\ \forall l \in L \text{ link prices updating} \end{cases} \quad (15)$$

where  $[\cdot]_+ \triangleq \max(\cdot, 0)$ ,  $\epsilon(m)$  is the step size,  $\bar{\theta}_l(m)$  is the average link rate measured by link  $l$  within the update interval  $T_m$ , and  $T_m$  is the time interval between the system updating  $(\mathbf{x}(m-1), \mathbf{r}(m-1))$  and  $(\mathbf{x}(m), \mathbf{r}(m))$ .

To make the time-scale separation assumption hold, we can choose properly decreasing step sizes and increasing update intervals. In this way, we make  $\mathbf{x}$  and  $\mathbf{r}$  change slowly to allow the designed Markov chain to approach its stationary distribution, and thus obtaining a good estimation of average link rate  $\sum_{h \in H} \lambda_{l,h} q_h$  for any  $l \in L$ . We have the following result:

**Theorem 2.** *Assume that  $U'_s(0) < \infty, \forall s \in S$ ,  $\max_{s,m} x_s(m) < \infty$  and  $\max_{l,m} r_l(m) < \infty$ . Then the stochastic primal-dual algorithm (15) converges to the optimal solutions of  $\mathbf{DP} - \beta$  (13) asymptotically with probability one under the following conditions on step sizes and update*

intervals:

$$T_m > 0 \quad \forall m \quad (16)$$

$$\epsilon(m) > 0 \quad \forall m, \quad \sum_{m=1}^{\infty} \epsilon(m) = \infty, \quad \sum_{m=1}^{\infty} \epsilon^2(m) < \infty \quad (17)$$

$$\sum_{m=1}^{\infty} \frac{\epsilon(m)}{T_m} < \infty \quad (18)$$

Further, the setting  $\epsilon(1) = T_1 = 1, \epsilon(m) = \frac{1}{m}, T_m = m, m \geq 2$  is one specific choice of step sizes and update intervals satisfying conditions (16)-(18). This setting depends only on the time index  $m$ , and thus can be generally applied to any network.

The proof is very similar to the proof in [18] and we omit details here. Intuitively, as  $T_m \rightarrow \infty$ , Markov chain is allowed to converge to its stationary distribution before  $\mathbf{x}(m)$  and  $\mathbf{r}(m)$  change. What is more, for any link  $l \in L$ , the time average of link rate  $\bar{\theta}_l(m)$  will approach the ensemble average of link rate  $\sum_{h \in H} \lambda_{l,h} q_h(\beta \mathbf{r}(m))$  because the underlying Markov chain is ergodic. On the other hand, accumulated estimation errors can be canceled by diminishing step sizes. Therefore, under properly-chosen decreasing step sizes and increasing update intervals, we have the separation of time scales of the dynamics of  $\mathbf{x}, \mathbf{r}$  and the designed Markov chain, and the stochastic primal-dual algorithm converges to optimal solution of  $\mathbf{DP} - \beta$  (13) with probability one.

Without time-scale separation, under constant step sizes and constant update intervals, we have the following convergence result:

**Theorem 3.** *Assume that  $U'_s(0) < \infty, \forall s \in S$ ,  $\max_{s,m} x_s(m) < \infty$  and  $\max_{l,m} r_l(m) < \infty$ . If the sequence of step size  $\{\epsilon(m)\}$  and the sequence of update interval  $\{T_m\}$  satisfy the following conditions:*

$$T_m = T_0 > 0 \quad \forall m \quad (19)$$

$$\epsilon(m) = \epsilon > 0 \quad \forall m \quad (20)$$

By running the stochastic primal-dual algorithm (15),  $(\mathbf{x}(m), \mathbf{r}(m))$  converges with probability one to the bounded neighborhood of  $\hat{\mathbf{x}}$  and  $\hat{\mathbf{r}}$ , i.e., optimal solutions of  $\mathbf{DP} - \beta$  (13) as follows:

$$\{(\mathbf{x}, \mathbf{r}) : |L_\beta(\mathbf{x}, \mathbf{r}) - L_\beta(\hat{\mathbf{x}}, \hat{\mathbf{r}})| \leq \frac{C_3}{T_0} + \epsilon \frac{(C_1 + C_2)}{2}\},$$

where  $C_1, C_2, C_3$  are positive constants.

The proof is relegated to Appendix-D.

Our emphasis on constant step sizes and constant update intervals has two reasons. First, a diminishing step size usually leads to slow convergence near the optimal solutions. Second, it is convenient to implement constant step sizes and constant update intervals in practice.

Inspired by and similar to [22], [46], we also adopt the standard methods of stochastic approximation [47], [48] and Markov chain [49], [50]. The difference between our proof and [22], [46] is that, our proof studies the saddle points of Lagrangian function, while [22], [46] studies the optimal dual solutions directly. Therefore, in general, our proof techniques

can be applied to primal-dual resource allocation algorithms, while proof techniques in [22], [46] can be applied only to dual resource allocation algorithms.

### E. Summary of Results and Discussion

In this subsection, first, we give a summary of results in Table I. Then we discuss the impacts of parameters  $\beta$  (approximation factor),  $T_0$  (update interval) and  $\epsilon$  (step size):

- **Impacts of  $\beta$  (approximation factor)** : The larger the value of  $\beta$ , the smaller the gap between log-sum-exp approximation and the max function, and the smaller the gap between the output of stochastic primal-dual algorithm and the optimal value. However, as discussed in [18], usually there are practical constraints or overhead concerns on using large values of  $\beta$ . What is more, for very large values of  $\beta$ , except possible multiple maximum independent sets, the stationary state probabilities of Markov chain ( $q_h(\beta\mathbf{r})$  in (10)) for all other independents will be almost zero. For multiple maximum independent sets, the probability is distributed evenly among these sets. Further, with very large values of  $\beta$ , starting from any initial state (independent set), the designed Markov chain will search its neighbor states and jump to a better state (larger independent set) with a probability close to 1. Therefore, this designed Markov chain is very likely to be trapped in a local maximal independent set (not maximum independent set). It will take a long time for this Markov chain to reach any one of maximum independent sets. Thus starting from any initial state, the time for this Markov chain to reach the stationary state will increase a lot.
- **Impacts of  $T_0$  (update interval)** : The larger the value of  $T_0$ , the smaller the gap between the ensemble average of link rates and the time average of link rates, *i.e.*, the smaller the estimation errors, and the smaller the gap between the output of stochastic primal-dual algorithm and the optimal value. However, the stochastic primal-dual algorithm converges slowly with large values of  $T_0$ .
- **Impacts of  $\epsilon$  (step size)** : The smaller the value of  $\epsilon$ , the more estimation errors are canceled, and the smaller the gap between the output of stochastic primal-dual algorithm and the optimal value.

## IV. NUM OVER GENERAL MULTI-HOP NETWORK: NODE-CENTRIC FORMULATION

In this section, we focus on the node-centric formulation based feasible rate region. There are several differences between the node-centric formulation and the link-centric formulation [5]. First, in the node-centric formulation, each user does *not* use any pre-specified set of paths, while in the link-centric formulation, each user uses a pre-specified set of paths. Second, the scheduling component of the node-centric formulation incorporates the routing functionality, while the scheduling component of the link-centric formulation does *not*. Third, the node-centric formulation does *not* require end-to-end feedback, while the link-centric formulation does (aggregate link prices along the paths).

In spite of these differences, the applications of Markov approximation framework to the node-centric formulation and the link-centric formulation are very similar. In the following, we state the results only and omit details of all proofs. We also omit the summary of results and the discussion of impacts of  $\beta$ ,  $T_0$  and  $\epsilon$  since they are also similar to their counterparts in link-centric formulation.

The wireless network is represented as a graph  $G = (\mathcal{N}, \mathcal{L})$ , where  $\mathcal{N}$  is the set of nodes, and  $\mathcal{L}$  is the set of links.  $S$  denotes the user set and  $\mathbf{x} = [x_s, s \in S]^T$  denotes the vector of sending rates of users.

Let  $H$  be the set of all independent sets over the corresponding conflict graph  $G_c$ . Let  $\mathbf{q} = [q_h, h \in H]^T$  be the vector of probability (or time fraction) of all independent sets. Let  $\lambda_{i,j,h}$  be the capacity of link  $(i, j)$  within the independent set  $h$ .  $\lambda_{i,j,h} = 0$  means link  $(i, j)$  is not activated within the independent set  $h$ .

Given a user  $s \in S$ , we let  $f_{i,j}^s$  denote the flow rate from source  $s$  to destination  $t_s$  over link  $l = (i, j)$ . Let

$$1_A = \begin{cases} 1 & \text{if event A is true} \\ 0 & \text{otherwise} \end{cases} \quad (21)$$

Then we consider the following master utility maximization problem:

$$\text{MPN} : \max_{\mathbf{x}, \mathbf{f}, \mathbf{q} \geq 0} \sum_{s \in S} U_s(x_s) \quad (22)$$

$$\text{s.t. } x_s 1_{i=s} + \sum_{j:(j,i) \in \mathcal{L}} f_{j,i}^s \leq \sum_{j:(i,j) \in \mathcal{L}} f_{i,j}^s, \forall i \in \mathcal{N} - \{t_s\}, s \in S \quad (23)$$

$$\sum_{s \in S} f_{i,j}^s \leq \sum_{h \in H} \lambda_{i,j,h} q_h, \quad \forall (i, j) \in \mathcal{L}, \quad (24)$$

$$\sum_{h \in H} q_h = 1. \quad (25)$$

Similar to the previous link-centric formulation, we apply the Markov approximation framework. Then we are actually solving a problem close to the original problem MPN:

$$\text{MPN} - \beta : \max_{\mathbf{x}, \mathbf{f}, \mathbf{q} \geq 0} \sum_{s \in S} U_s(x_s) - \frac{1}{\beta} \sum_{h \in H} q_h \log q_h \quad (26)$$

$$\text{s.t. } x_s 1_{i=s} + \sum_{j:(j,i) \in \mathcal{L}} f_{j,i}^s \leq \sum_{j:(i,j) \in \mathcal{L}} f_{i,j}^s, \forall i \in \mathcal{N} - \{t_s\}, s \in S \quad (27)$$

$$\sum_{s \in S} f_{i,j}^s \leq \sum_{h \in H} \lambda_{i,j,h} q_h, \quad \forall (i, j) \in \mathcal{L}, \quad (28)$$

$$\sum_{h \in H} q_h = 1. \quad (29)$$

where  $\beta$  is a positive constant.

Associated the first set of inequality constraints (27) with Lagrange multipliers  $\mathbf{r} = [r_i^s, s \in S, i \in \mathcal{N}]^T$ , where  $r_{t_s}^s = 0, \forall s \in S$ . By using standard Lagrange dual decomposition method, we can show that solving the problem MPN -  $\beta$  (26) is equal to finding the saddle point of the following problem

$$\text{DDPN} - \beta : \min_{\mathbf{r} \geq 0} \max_{\mathbf{x} \geq 0} L_\beta(\mathbf{x}, \mathbf{r}) \quad (30)$$

TABLE I  
SUMMARY OF RESULTS FOR OUR LINK-CENTRIC FORMULATION

	NUM	Scheduling
Original Problems	Master Problem <b>MP</b> (2) with optimal solution $\mathbf{x}^*$ .	Maximum Weighted Independent Set (MWIS) Problem (5) with corresponding optimal distribution for independent sets (6): $q_h = \frac{1}{ H^* }, \forall h \in H^*; q_h = 0, \forall h \in H - H^*$ .
Approximated Problems	Approximated Problem <b>MP</b> $-\beta$ (11) with optimal solution $\hat{\mathbf{x}}$ . Equivalent approximated problem <b>DP</b> $-\beta$ (13) with optimal solution $(\hat{\mathbf{x}}, \hat{\mathbf{r}})$ . We also have $ \sum_{s \in S} (U_s(\hat{x}_s) - U_s(x_s^*))  \leq \frac{\log  H }{\beta}$ . (12)	Approximated MWIS problem <b>MWIS</b> $-\beta$ (9). Corresponding optimal distribution for independent sets: $\forall h \in H, q_h(\beta \mathbf{r}) = \frac{\exp(\beta \sum_{l \in L} \lambda_{l,h} r_l)}{\sum_{h \in H} \exp(\beta \sum_{l \in L} \lambda_{l,h} r_l)}$ (10)
Our Distributed Algorithms Solving the Approximated Problems: decreasing step sizes and increasing update intervals (16)-(18)	Stochastic primal-dual algorithm (15) converges to $(\hat{\mathbf{x}}, \hat{\mathbf{r}})$ with probability one (time-scale separation holds)	Algorithm 1 schedules link transmissions and implicitly implements a Markov chain over all independent sets $H$ . The stationary distribution of this Markov chain is $q_h(\beta \mathbf{r})$ in (10), $\forall h \in H$ .
Our Distributed Algorithms Solving the Approximated Problems: constant step sizes and constant update intervals	Stochastic primal-dual algorithm (15) converges with probability one to the bounded neighborhood of $(\hat{\mathbf{x}}, \hat{\mathbf{r}})$ as follows: $\{(\mathbf{x}, \mathbf{r}) :  L_\beta(\mathbf{x}, \mathbf{r}) - L_\beta(\hat{\mathbf{x}}, \hat{\mathbf{r}})  \leq \frac{C_3}{T_0} + \epsilon \frac{(C_1 + C_2)}{2}\}$	Algorithm 1 schedules link transmissions and implicitly implements a Markov chain over all independent sets $H$ . The stationary distribution of this Markov chain is $q_h(\beta \mathbf{r})$ in (10), $\forall h \in H$ .

where

$$L_\beta(\mathbf{x}, \mathbf{r}) = \sum_{s \in S} [U_s(x_s) - r_s^s x_s] + \frac{1}{\beta} \log \left[ \sum_{h \in H} \exp(\beta \sum_{(i,j) \in \mathcal{L}} \lambda_{i,j,h} w_{i,j}) \right], \quad (31)$$

$$w_{i,j} = \max_{s \in S} [r_i^s - r_j^s]_+, \quad \forall (i,j) \in \mathcal{L}. \quad (32)$$

The corresponding (unique) optimal solution of  $q_h(\beta \mathbf{r}), h \in H$  is

$$q_h(\beta \mathbf{r}) = \frac{\exp(\beta \sum_{(i,j) \in \mathcal{L}} \lambda_{i,j,h} w_{i,j})}{\sum_{h' \in H} \exp(\beta \sum_{(i,j) \in \mathcal{L}} \lambda_{i,j,h'} w_{i,j})}, \quad \forall h \in H. \quad (33)$$

We explore algorithm design in the following subsections. The  $q_h(\beta \mathbf{r}), h \in H$  in (33) can be interpreted as the stationary distribution of a time reversible Markov chain, whose states are the independent sets in  $H$ . We first discuss how to design and implement such a Markov chain in a distributed manner, then we design primal-dual algorithms to solve the problem **DDPN**  $-\beta$ .

#### A. Design and Implementation of Markov Chain

The design method of Markov chain, corresponding pseudocode and related proof are very similar to their counterparts for link-centric formulation in Section III-B. Therefore we omit them for clarity.

#### B. Solving the Approximated Problem by the Primal-Dual Algorithm

Since  $L_\beta(\mathbf{x}, \mathbf{r})$  is not differential with respect to  $\mathbf{r}$ , we need to use the corresponding sub-gradients. In the following, we propose a primal-dual algorithm to solve .

Denote the user (source) rates as  $x_s, s \in S$  and the node prices as  $r_i^s, s \in S$ . To solve the problem **DDPN**  $-\beta$ ,

we propose a primal-dual subgradient based flow control algorithm and associated scheduling policy as follows:

*Flow-Control:* The primal-dual flow-control algorithm is given as follows:

$$\begin{cases} \dot{x}_s = \alpha_s [U'_s(x_s) - r_s^s]_{x_s}^+ \\ \forall s \in S, \text{ user rates updating} \\ \dot{r}_i^s = k_i^s \left[ x_s \mathbf{1}_{i=s} + \sum_{j:(j,i) \in \mathcal{L}} f_{j,i}^s - \sum_{j:(i,j) \in \mathcal{L}} f_{i,j}^s \right]_{r_i^s}^+ \\ \forall i \in \mathcal{N} - \{t_s\}, s \in S, \text{ non-destination node prices updating} \\ \dot{r}_{t_s}^s = r_{t_s}^s = 0, \forall s \in S, \text{ destination node prices updating} \end{cases}, \quad (34)$$

where  $k_i^s (i \in \mathcal{N} - \{t_s\}, s \in S)$  and  $\alpha_s (s \in S)$  are positive constants, and function

$$[b]_a^+ = \begin{cases} \max(0, b) & a \leq 0 \\ b & a > 0 \end{cases}$$

*Scheduling:* for each link  $(i,j) \in \mathcal{L}$ , find the user  $s_{i,j}^*$  such that

$$s_{i,j}^* = \arg \max_{s \in S} (r_i^s - r_j^s), \quad (35)$$

and the link transmission rate is defined as follows:

$$f_{ij}^s = \begin{cases} \sum_{h \in H} \lambda_{i,j,h} q_h & \text{if } s = s_{i,j}^*, \text{ and } w_{i,j} > 0 \\ 0 & \text{otherwise} \end{cases} \quad (36)$$

When the link  $(i,j)$  gets opportunity to transmit, if  $w_{i,j} > 0$ , it will serve flows of the user  $s_{i,j}^*$  with the service rate  $\sum_{h \in H} \lambda_{i,j,h} q_h$ ; otherwise, it will transmit NULL bits.

Note that  $w_{i,j}$  represents the maximum differential backlog between nodes and (maximized over all users). The policy thus uses back-pressure in an effort to equalize differential backlogs. We emphasize that this scheme does not require knowledge of the arrival rates or channel statistics, and does

not use any pre-specified set of routes. The route for each unit of data is found dynamically.

### C. Convergence Properties

We use  $\mathbf{x}^*$  and  $\hat{\mathbf{x}}$  to denote the optimal user rates of master problem MPN (22) and problem MPN  $-\beta$  (26) respectively. Then we can see that

$$\sum_{s \in S} U_s(\hat{x}_s) \leq \sum_{s \in S} U_s(x_s^*) \leq \sum_{s \in S} U_s(\hat{x}_s) + \frac{1}{\beta} \log |H|. \quad (37)$$

As  $\beta \rightarrow \infty$ ,  $\hat{\mathbf{x}} \rightarrow \mathbf{x}^*$ .

With the time-scale separation assumption that Markov chain converges to its stationary distribution instantaneously compared to the time-scale of adaption of the Markov chain parameters, we have the following result:

**Theorem 4.** *The primal-dual algorithm (34) is globally asymptotically stable.*

Without the time-scale separation assumption on Markov chain, in practice, we have the following stochastic primal-dual algorithm:

$$\begin{cases} x_s(m+1) = [x_s(m) + \epsilon(m)(U'_s(x_s(m)) - r_s^s(m))]_+, \forall s \in S \\ \text{user rates updating} \\ r_i^s(m+1) = [r_i^s(m) + \epsilon(m)z_i^s(m)]_+, \forall i \in \mathcal{N} - \{t_s\}, s \in S \\ \text{Non-destination node prices updating} \\ r_{t_s}^s(m+1) = r_{t_s}^s(m) = 0, \forall s \in S \\ \text{destination node prices updating} \end{cases} \quad (38)$$

where  $\forall i \in \mathcal{N}, s \in S, m$ ,

$$z_i^s(m) = x_s(m)1_{i=s} + \sum_{j:(j,i) \in \mathcal{L}} \bar{f}_{j,i}^s(m) - \sum_{j:(i,j) \in \mathcal{L}} \bar{f}_{i,j}^s(m),$$

$\epsilon(m)$  is the step size, and  $\bar{f}_{i,j}^s(m)$  is the average flow rate of user  $s$  over link  $(i, j)$  measured within the update interval  $T_m$ .

Similar to the link-centric formulation, we have the following convergence result of the stochastic primal-dual algorithm (38):

**Theorem 5.** *Assume that  $U'_s(0) < \infty, \forall s \in S$ ,  $\max_{s,m} x_s(m) < \infty$  and  $\max_{i,m} r_i^s(m) < \infty$ . If the sequence of step size  $\{\epsilon(m)\}$  and the sequence of update interval  $\{T_m\}$  satisfy the following conditions:*

$$T_m > 0 \quad \forall m \quad (39)$$

$$\epsilon(m) > 0 \quad \forall m, \quad \sum_{m=1}^{\infty} \epsilon(m) = \infty, \quad \sum_{m=1}^{\infty} \epsilon^2(m) < \infty \quad (40)$$

$$\sum_{m=1}^{\infty} \frac{\epsilon(m)}{T_m} < \infty \quad (41)$$

By running the stochastic primal-dual algorithm (38),  $(\mathbf{x}(m), \mathbf{r}(m))$  converges to  $(\hat{\mathbf{x}}, \hat{\mathbf{r}})$  with probability one. Further, the setting  $\epsilon(1) = T_1 = 1, \epsilon(m) = \frac{1}{m}, T_m = m, m \geq 2$  is one specific choice of step sizes and update intervals satisfying conditions (39)-(41). This setting depends only on the index  $m$ , and thus can be generally applied to any network.

**Theorem 6.** *Assume that  $U'_s(0) < \infty, \forall s \in S$ ,  $\max_{s,m} x_s(m) < \infty$  and  $\max_{i,m} r_i^s(m) < \infty$ . If the sequence of step size  $\{\epsilon(m)\}$  and the sequence of update interval  $\{T_m\}$  satisfy the following conditions:*

$$T_m = T_0 > 0 \quad \forall m \quad (42)$$

$$\epsilon(m) = \epsilon > 0 \quad \forall m \quad (43)$$

By running the stochastic primal-dual algorithm (38),  $(\mathbf{x}(m), \mathbf{r}(m))$  converges with probability 1 to the bounded neighborhood of  $\hat{\mathbf{x}}$  and  $\hat{\mathbf{r}}$  as follows:

$$\{(\mathbf{x}, \mathbf{r}) : |L_\beta(\mathbf{x}, \mathbf{r}) - L_\beta(\hat{\mathbf{x}}, \hat{\mathbf{r}})| \leq \frac{C'_3}{T_0} + \epsilon \frac{(C'_1 + C'_2)}{2}\},$$

where  $C'_1, C'_2, C'_3$  are positive constants.

## V. NUMERICAL EXAMPLES

In this section, we present numerical experiments to illustrate the performance of the stochastic primal-dual algorithms under constant step sizes and constant update intervals for both link-centric formulation and node-centric formulation. We consider proportional fairness, *i.e.*, the utility function is a log function. The performance metrics that we focus on are individual user's rates and aggregate user utilities.

In the following, first, we examine the convergence performance of the stochastic primal-dual algorithm proposed in (15) and (38) respectively. The numerical results are shown to converge to a small neighborhood of the optimal solutions of wireless NUM problem. Second, we compare the numerical results with theoretical results obtained by treating interference as noise. It turns out we achieve smaller aggregate utilities as well as smaller user rates by treating interference as noise. Third, we study the impacts of  $\beta$  (approximation factor),  $T_0$  (update interval) and  $\epsilon$  (step size) on the convergence performance of the stochastic primal-dual algorithms. We will see that with a larger  $\beta$ , a larger  $T_0$  and a smaller  $\epsilon$ , we obtain a smaller gap between numerical results and optimal solutions of wireless NUM problem. Intuitively, we obtain a smaller gap because a larger  $\beta$  increases the approximation accuracy of log-sum-exp approximation, a larger  $T_0$  reduces the estimation errors caused by replacing the expectation of link rates with a time-average of link rates, and a smaller  $\epsilon$  reduces the estimation errors too. Fourth, we study the impacts of  $\beta$  on convergence time of the stochastic primal-dual algorithm (15).

### A. Link-centric Formulation

We consider a network scenario shown in Fig. 8, where user 1 chooses the path  $A \rightarrow B \rightarrow C$ , user 2 chooses the path  $B \rightarrow C \rightarrow G$ , user 3 chooses the path  $D \rightarrow E \rightarrow F$ , and user 4 chooses the path  $E \rightarrow F \rightarrow G$ . By focusing on proportional-fairness, we choose utility function  $U(\cdot) = \log(\cdot + 0.1)$ . By running the primal-dual algorithm (15) with constant step size  $\epsilon = 0.01$ , constant update interval  $T_0 = 100$  and approximating factor  $\beta = 100$ , we have the corresponding rates and prices shown in Fig. 9 and Fig. 10 respectively. We compare the numerical results with theoretically optimal values in Table II.

**Advantage of Deterministic Channel Model Over Treating Interference As Noise:** By treating interference as noise (TIAN), we can only obtain aggregate utilities  $-0.8310$  (maximum in theory) and user rates  $1, 0.5, 1, 0.5$  (maximum in theory). In contrast, by deterministic channel model and **not** treating interference as noise, we obtain larger aggregate utilities  $-0.0816$  (maximum in theory), as well as larger user rates  $1.5, 0.5, 1.5, 0.5$  (maximum in theory). Further, by running our primal-dual algorithms, we obtain aggregate utilities  $-0.08136$  and user rates  $1.5, 0.5, 1.5, 0.5$ . The numerical results are close to the optimal solutions with **not** treating interference as noise, all within 2.45% of the optimal values. Therefore, numerical results illustrate the convergence and optimality of our joint scheduling and primal-dual flow control algorithms.

**Impacts of  $\beta$ ,  $T_0$  and  $\epsilon$  on Rates and Utilities:** Now for three parameters  $\beta$ ,  $T_0$  and  $\epsilon$ , we fix any two of them and study the impacts of the remaining one on user rates and aggregate user utilities. We omit studies on link prices because the observations are very similar. We run the primal-dual algorithm (15) for 1000 iterations and corresponding numerical results on  $\beta$ ,  $T_0$  and  $\epsilon$  are shown in Table III, Table IV and Table V respectively. We can see that

- As  $\beta$  decreases, the gap between the numerical result and the optimal value is *increasing*, though not monotonically increasing for all flow rates. Too small  $\beta$  results in deterioration of performance.
- As  $T_0$  decreases, the gap between the numerical result and the optimal value is *increasing*, though not monotonically increasing for all flow rates. Too small  $T_0$  results in deterioration of performance.
- As  $\epsilon$  increases, the gap between the numerical result and the optimal value is *increasing*, though not monotonically increasing for all flow rates.

Next, we study the impacts of  $\beta$  on convergence time.

**Impacts of  $\beta$  on Convergence Time:** We fix values of update interval  $T_0$  and step size  $\epsilon$ , and study the impacts of  $\beta$  on convergence time. The convergence time is defined as the length of update interval *times* the number of iterations needed to converge. Since the update interval  $T_0$  is fixed, we are concerned with the number of iterations needed to converge. We focus on the user rates and omit the prices because the observations are very similar. Numerical results are shown in Table VI. We observe that there are no simply increasing or decreasing relationships between the convergence time of the stochastic primal-dual algorithm (15) and  $\beta$ . In fact, the converge time of the primal-dual algorithm (15) depends mainly on the update interval  $T_0$  and step size  $\epsilon$ . Too large values of  $T_0$  and too small values of  $\epsilon$  cause a very slow convergence.

## B. Node-centric Formulation

We consider a butterfly network with three users shown in Fig. 11. We choose utility function of user 1, 2 and 3 to be  $U(\cdot) = \log(\cdot+0.1)$ ,  $U(\cdot) = \log(\cdot+0.3)$  and  $U(\cdot) = \log(\cdot+0.5)$  respectively. By running the primal-dual algorithm (15) with constant step size  $\epsilon = 0.05$ , constant update interval  $T_0 = 100$  and approximating factor  $\beta = 100$ , we have the corresponding

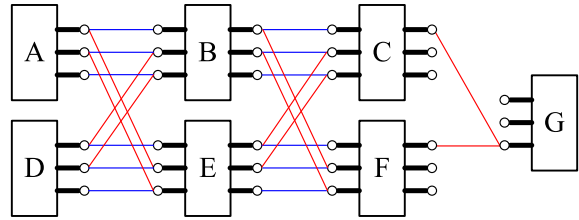


Fig. 8. A wireless deterministic network with channel gains  $\rho_{AB} = \rho_{BC} = \rho_{DE} = \rho_{EF} = 3$ ,  $\rho_{AE} = \rho_{DB} = \rho_{BF} = \rho_{EC} = 2$ , and  $\rho_{CG} = \rho_{FG} = 1$ . Four users are associated with paths  $A \rightarrow B \rightarrow C$ ,  $B \rightarrow C \rightarrow G$ ,  $D \rightarrow E \rightarrow F$ , and  $E \rightarrow F \rightarrow G$  respectively.

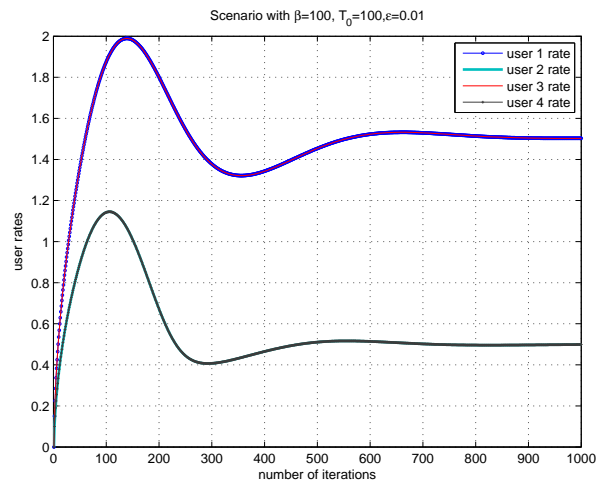


Fig. 9. Performance of the primal-dual algorithm on user rates with  $\beta = 100$ ,  $T_0 = 100$ ,  $\epsilon = 0.01$ . Initial values of user rates are all 0. Because of symmetry, not only rate of user 1 and rate of user 3 evolves nearly in the same way, but also rate of user 2 and rate of user 4 evolves nearly in the same way.

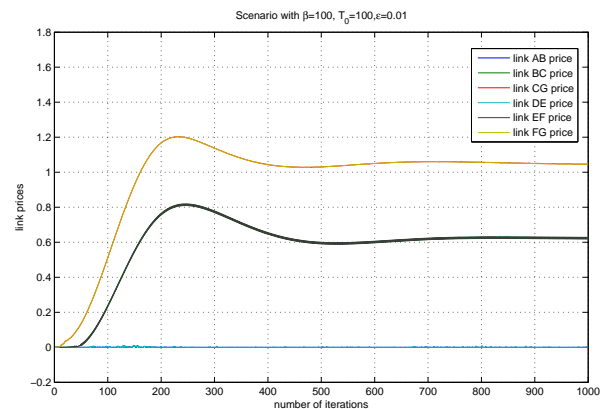


Fig. 10. Performance of the primal-dual algorithm on link prices with  $\beta = 100$ ,  $T_0 = 100$ ,  $\epsilon = 0.01$ . Initial values of link prices are all 0. Because of symmetry, price pairs such as price of Link AB and price of Link DE, price of Link BC and price of Link EF, price of Link CG and price of Link FG, evolve nearly in the same way respectively.

TABLE II  
PERFORMANCE COMPARISON WITH  $\beta = 100, T_0 = 100, \epsilon = 0.01$ . HERE 'TIAN' DENOTES 'TREATING INTERFERENCE AS NOISE'.

	TIAN	Optimal	Approximation	Gap	Relative Error
Sum of Utility	-0.8310	-0.0816	-0.0836	0.0020	2.45%
Rate of User 1	1.0000	1.5000	1.5004	0.0004	0.03%
Rate of User 2	0.5000	0.5000	0.4992	0.0008	0.16%
Rate of User 3	1.0000	1.5000	1.5004	0.0004	0.03%
Rate of User 4	0.5000	0.5000	0.4993	0.0007	0.14%
Price of Link AB	0.0000	0.0000	0.0005	0.0005	
Price of Link BC	0.9091	0.6250	0.6191	0.0059	0.94%
Price of Link CG	0.7576	1.0417	1.0442	0.0025	0.24%
Price of Link DE	0.0000	0.0000	0.0006	0.0006	
Price of Link EF	0.9091	0.6250	0.6292	0.0042	0.67%
Price of Link FG	0.7576	1.0417	1.0434	0.0017	0.16%

TABLE III  
PERFORMANCE COMPARISON WITH  $T_0 = 100, \epsilon = 0.01$

	Optimal	$\beta = 100$	$\beta = 50$	$\beta = 10$	$\beta = 1$
Sum of Utility	-0.0816	-0.0836	-0.0827	-0.0922	-0.5573
Rate of User 1	1.5000	1.5004	1.5016	1.5046	1.6678
Rate of User 2	0.5000	0.4992	0.4990	0.4950	0.3275
Rate of User 3	1.5000	1.5004	1.5017	1.5044	1.6747
Rate of User 4	0.5000	0.4993	0.4991	0.4954	0.3271

TABLE IV  
PERFORMANCE COMPARISON WITH  $\beta = 100, \epsilon = 0.01$

	Optimal	$T_0 = 100$	$T_0 = 50$	$T_0 = 10$	$T_0 = 1$
Sum of Utility	-0.0816	-0.0836	-0.0783	-0.0551	0.3430
Rate of User 1	1.5000	1.5004	1.5032	1.5117	1.665
Rate of User 2	0.5000	0.4992	0.4999	0.5034	0.5712
Rate of User 3	1.5000	1.5004	1.5031	1.5125	1.6685
Rate of User 4	0.5000	0.4992	0.4998	0.5035	0.5714

user rates and node prices shown in Fig. 12 and Fig. 13 respectively. Focusing on user rates, we compare the numerical results with theoretically optimal values in Table VII. The numerical results of all users rates converge to the optimal solutions, all within 2.58% of the optimal values. We omit studies on node prices since the observations are very similar.

Now for three parameters  $\beta$ ,  $T_0$  and  $\epsilon$ , we fix two of them at a time and study the impacts of the remaining one on user rates. We run the primal-dual algorithm (15) for 1000 iterations. The numerical results on  $\beta$ ,  $T_0$  and  $\epsilon$  are

TABLE V  
PERFORMANCE COMPARISON WITH  $\beta = 100, T_0 = 100$

	Optimal	$\epsilon = 0.01$	$\epsilon = 0.02$	$\epsilon = 0.05$	$\epsilon = 0.1$
Sum of Utility	-0.0816	-0.0836	-0.0781	-0.0766	-0.0755
Rate of User 1	1.5000	1.5004	1.5016	1.5010	1.5030
Rate of User 2	0.5000	0.4992	0.5007	0.5004	0.5042
Rate of User 3	1.5000	1.5004	1.5012	1.5009	1.5001
Rate of User 4	0.5000	0.4992	0.5004	0.5020	0.4984

TABLE VI  
CONVERGENCE TIME (NUMBER OF ITERATIONS) WITH  
 $T_0 = 100, \epsilon = 0.01$

	$\beta = 200$	$\beta = 100$	$\beta = 50$	$\beta = 20$	$\beta = 10$
Rate of User 1	937	903	890	919	980
Rate of User 2	784	854	881	750	968
Rate of User 3	940	901	891	922	981
Rate of User 4	785	852	884	751	969

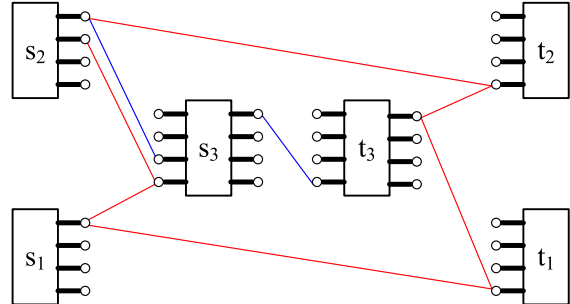


Fig. 11. A wireless butterfly network with channel gains  $\rho_{s_1 s_3} = \rho_{s_1 t_1} = 1$ ,  $\rho_{s_2 s_3} = 2$ ,  $\rho_{s_2 t_2} = 1$ ,  $\rho_{s_3 t_3} = 1$ , and  $\rho_{t_3 t_2} = \rho_{t_3 t_1} = 1$ . There are three users (source-destination pairs): user 1 ( $s_1, t_1$ ), user 2 ( $s_2, t_2$ ) and user 3 ( $s_3, t_3$ ).

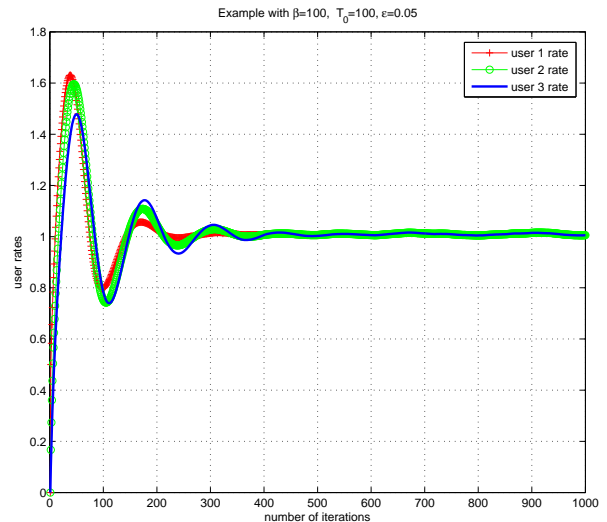


Fig. 12. Performance of the primal-dual algorithm on user rates with  $\beta = 100, T_0 = 100, \epsilon = 0.05$ . Initial values of all user rates are 0. All user rates converge to the neighborhood of 1, the optimal value.

shown in Table VIII, Table IX and Table X respectively. The observations are similar to the counterparts for Link-centric formulation and we omit them for clarity. We also omit the study for the impacts of  $\beta$  on convergence time.

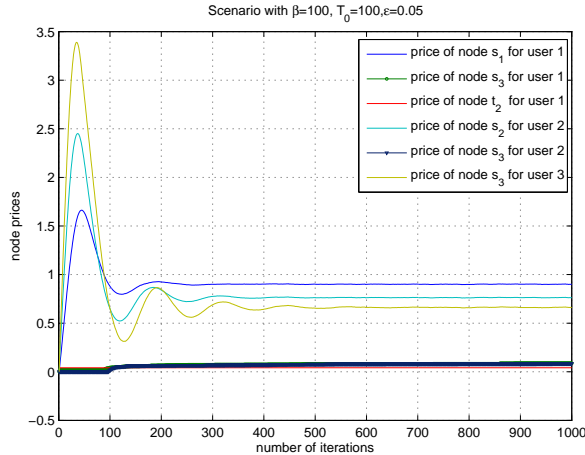


Fig. 13. Performance of the primal-dual algorithm on node prices with  $\beta = 100, T_0 = 100, \epsilon = 0.05$ . Initial values of all node prices for user 1, 2, 3 are 0. For convenience, we only show non-zero node prices. All other node prices not shown in this picture are 0 all the time.

TABLE VII

PERFORMANCE COMPARISON WITH  $\beta = 100, T_0 = 100, \epsilon = 0.05$ 

	Optimal	Approximation	Gap	Relative Error
Sum of Utility	0.7631	0.7800	0.0197	2.58%
Rate of User 1	1.0000	1.0076	0.0076	0.76%
Rate of User 2	1.0000	1.0070	0.0070	0.70%
Rate of User 3	1.0000	1.0070	0.0070	0.70%

TABLE VIII

PERFORMANCE COMPARISON WITH  $T_0 = 100, \epsilon = 0.05$ 

	Optimal	$\beta = 100$	$\beta = 50$	$\beta = 10$	$\beta = 1$
Sum of Utility	0.7631	0.7800	0.7880	0.7896	-0.1577
Rate of User 1	1.0000	1.0076	1.0107	1.0131	0.9118
Rate of User 2	1.0000	1.0070	1.0108	1.0133	0.9072
Rate of User 3	1.0000	1.0070	1.0104	1.0068	0.1992

TABLE IX

PERFORMANCE COMPARISON WITH  $\beta = 100, \epsilon = 0.05$ 

	Optimal	$T_0 = 100$	$T_0 = 50$	$T_0 = 10$	$T_0 = 1$
Sum of Utility	0.7631	0.7800	0.8086	0.9510	1.6322
Rate of User 1	1.0000	1.0076	1.0195	1.0826	1.4285
Rate of User 2	1.0000	1.0070	1.0197	1.0823	1.4106
Rate of User 3	1.0000	1.0070	1.0195	1.0833	1.4563

TABLE X

PERFORMANCE COMPARISON WITH  $\beta = 100, T_0 = 100$ 

	Optimal	$\epsilon = 0.05$	$\epsilon = 0.08$	$\epsilon = 0.1$	$\epsilon = 0.2$
Sum of Utility	0.7631	0.7800	0.7869	0.7882	0.7919
Rate of User 1	1.0000	1.0076	1.0103	1.0113	1.0125
Rate of User 2	1.0000	1.0070	1.0107	1.0110	1.0125
Rate of User 3	1.0000	1.0070	1.0094	1.0097	1.0119

## VI. CONCLUSIONS

In this paper, within the NUM framework, we study the cross-layer optimization problem for wireless networks with deterministic channel models. We present an extended conflict graph model to characterize the feasible rate region. In the important cases such as single-hop multiple access wireless networks, we show that the feasible rate region is equal to the information theoretic capacity region. Then we consider general multi-hop wireless networks with both link-centric formulation and node-centric formulation. We approximately solve the NUM problem in a distributed manner by Markov approximation framework, including the scheduling algorithm and primal-dual flow-control algorithm. The overall solution is shown to converge to the optimal solutions of the NUM problem with or without time-scale separation assumption. Further, we show the convergence to the bounded neighborhood of optimal solutions with probability one under constant step sizes and constant update intervals. Numerical results illustrate not only the advantage of deterministic channel model over treating interference as noise, but also the convergence and optimality of our joint scheduling and primal-dual flow control algorithms.

## APPENDIX

## A. Deterministic Multiple-access Channel

We have the following result:

**Proposition 4.** *For single-hop multiple access networks with deterministic channel model, the conflict graph based rate region is equal to the information-theoretic capacity region.*

*Proof:* For a single-hop multiple access network, there are  $N$  users communicate to a single receiver. For each user  $j \in S = \{1, \dots, N\}$ , let  $\rho_j$  denote channel gain of the channel from the user  $j$  to the receiver.

On one hand, let  $C_{MAC}$  denote the information-theoretic capacity region for this single-hop multiple access network, then by [2], we have

$$C_{MAC} = \left\{ \mathbf{x} : \sum_{j \in M} x_j \leq \max_{j \in M} \rho_j, \forall M \subseteq \{1, \dots, N\} \right\}$$

Note that this region is characterized by  $2^N - 1$  constraints, each corresponding to a nonempty subset of users.

On the other hand, let  $R_{MAC}$  denote the conflict graph based rate region for this single-hop multiple access network. Let  $L_s$  be the set of sub-links from source node  $s$  to the common receiver. Each sub-link in graph  $G$  have unit capacity. Let  $H$  be the set of all independent sets over conflict graph  $G_c$ . Let  $\mathbf{q} = [q_h, h \in H]^T$  be the vector of probability (or time fraction) of all independent sets. Then we have

$$R_{MAC} = \bigcup_{\mathbf{q} \in \mathcal{Q}} R_{\mathbf{q}}$$

where

$$\mathcal{R}(\mathbf{q}) = \left\{ \mathbf{x} : x_s \leq \sum_{l \in L_s} \sum_{h: l \in h} q_h, \forall s \in S = \{1, \dots, N\} \right\}$$

and

$$\mathcal{Q} = \left\{ \mathbf{q} : \sum_{h \in H} q_h \leq 1, q_h \geq 0, \forall h \in H \right\}$$

We will show that any set of rates achievable in  $R_{MAC}$  is also achievable in  $C_{MAC}$ , and *vice versa*.

First, we have  $R_{MAC} \subseteq C_{MAC}$  since conflict graph model uses only a subset of possible information-theoretic schemes to achieve the rate region.

Second, we will show that  $C_{MAC} \subseteq R_{MAC}$ . The capacity region  $C_{MAC}$  is a  $N$ -dimensional polyhedron, and successive decoding with interference cancelation can achieve all corner points of  $C_{MAC}$  [2], [9]. Every decoding order corresponds to a different corner point of  $C_{MAC}$ , and consequently, there are  $N!$  corner points in the capacity region  $C_{MAC}$ . By the convexity of  $C_{MAC}$  and  $R_{MAC}$  (due to the convex hull operation), it is sufficient to show that all corner points (i.e., the successive decoding points) of  $C_{MAC}$  are in the capacity region  $R_{MAC}$ .

Given a decoding order  $\pi_1, \pi_2, \dots, \pi_N$  in which user  $\pi_1$  is decoded first, user  $\pi_2$  is decoded second,  $\dots$ , user  $\pi_N$  is decoded last. Without loss of generality, we assume that  $\rho_{\pi_1} \leq \rho_{\pi_2} \leq \dots \leq \rho_{\pi_N}$ , then the rate vector of the corresponding corner point  $\mathbf{x}(\pi)$  is equal to

$$\begin{aligned} x_{\pi_1} &= \rho_{\pi_1} \\ x_{\pi_2} &= \rho_{\pi_2} - \rho_{\pi_1} \\ &\vdots \\ x_{\pi_N} &= \rho_{\pi_N} - \rho_{\pi_{N-1}} \end{aligned}$$

Now we will show  $\mathbf{x}(\pi) \in R_{MAC}$ . We construct an independent set  $H_\pi$  of the corresponding conflict graph, which includes  $\rho_1$  sub-links of user  $\pi_1$ ,  $\rho_2 - \rho_1$  sub-links of user  $\pi_2$ ,  $\dots$ ,  $\rho_{\pi_N} - \rho_{\pi_{N-1}}$  sub-links of user  $\pi_N$ . Sub-links belonging to different users are disjoint. Also we let probability (or time fraction) of this independent set  $q_{H_\pi} = 1$ , thus the probability of all other independent sets are zero. Then we can see that for any user  $\pi_j$ ,  $j \in \{1, 2, \dots, N\}$ ,  $x_{\pi_j} = (\rho_{\pi_j} - \rho_{\pi_{j-1}}) q_{H_\pi} = \rho_{\pi_j} - \rho_{\pi_{j-1}}$ .

Thus  $\mathbf{x}(\pi) \in R_{MAC}$ . Similarly, all corner points (i.e., the successive decoding points) of  $C_{MAC}$  are in the capacity region  $R_{MAC}$ . Therefore,  $C_{MAC} \subseteq R_{MAC}$ . Combining two directions, we have  $C_{MAC} = R_{MAC}$ . ■

### B. Proof of Proposition 3

First, let state 0 denote the state where no link is transmitting. Since direct transitions are allowed only between two ‘‘adjacent’’ states that differ by one and only one link configuration, it is not hard to verify that state 0 can reach any other state in a finite number of transitions and vice versa. Therefore, all two states  $h, h'$  can reach each other within a finite number of transitions, either by direct transitions (if  $h$  and  $h'$  are adjacent states), or  $h(h')$  reaches 0 first, then starts from 0 to reach  $h'(h)$ . Therefore, the constructed Markov chain is irreducible. Further, it is a finite state ergodic Markov chain with a unique stationary distribution. We now show that the stationary distribution is indeed (10).

According to the Algorithm 1, only one link and only one of its configurations can be activated at a time. Thus direct transitions occur only between two ‘‘adjacent’’ states. Denote this link configuration as  $l_k$ , which belongs to  $\frac{\rho_l(\rho_l+1)}{2}$  configurations of link  $l$ . Now given any two adjacent states  $h$  and  $h'$  where  $|h| = |h'| \cup \{l_k\}$ . Since the timer for link configuration  $l_k$  counters down according to an exponential distribution with rate  $\lambda_{l_k,h} \exp(\beta \lambda_{l_k,h} r_l)$ , we have  $q_{h',h} = \lambda_{l_k,h} \exp(\beta \lambda_{l_k,h} r_l)$ . On the other hand, transmit time of  $l_k$  follows an exponential distribution with rate  $\lambda_{l_k,h}$ , thus  $q_{h,h'} = \lambda_{l_k,h}$ .

With (10), we have  $q_h(\beta \mathbf{r}) \cdot q_{h,h'} = q_{h'}(\beta \mathbf{r}) \cdot q_{h,h}$ , i.e., the detailed balance equations hold. For any two non-adjacent states, the detailed balance equations hold trivially. Thus the constructed Markov chain is time-reversible and its stationary distribution is indeed (10) according to Theorem 1.3 and Theorem 1.14 in [45].

### C. Proof of Theorem 1

Let  $\hat{x}_s (s \in S)$  and  $\hat{r}_l (l \in L)$  be the optimal solutions of the problem  $\mathbf{DP} - \beta$  (13). Since the log-sum-exponential function in (13) is convex with respect to  $\mathbf{r}$  [43], thus  $L_\beta(\mathbf{x}, \mathbf{r})$  is concave in  $\mathbf{x}$  and convex in  $\mathbf{r}$ . By properties of gradients for convex functions [43], we have

$$\begin{aligned} (\hat{\mathbf{x}} - \mathbf{x})^T \cdot \nabla_{\mathbf{x}} L_\beta(\mathbf{x}, \mathbf{r}) &\geq 0 \\ (\hat{\mathbf{r}} - \mathbf{r})^T \cdot \nabla_{\mathbf{r}} L_\beta(\mathbf{x}, \mathbf{r}) &\leq 0 \end{aligned}$$

Thus

$$\sum_{s \in S} (\hat{x}_s - x_s) \left[ U'_s(x_s) - \sum_{l: l \in S} r_l \right] \geq 0 \quad (44)$$

$$\sum_{l \in L} (\hat{r}_l - r_l) \left[ \sum_{h \in H} \lambda_{l,h} q_h(\beta \mathbf{r}) - \sum_{s: l \in S} x_s \right] \leq 0 \quad (45)$$

Consider the following Lyapunov function

$$V(\mathbf{x}, \mathbf{r}) = \sum_{s \in S} \int_{\hat{x}_s}^{x_s} \frac{1}{\alpha_s} (v - \hat{x}_s) dv + \sum_{l \in L} \int_{\hat{r}_l}^{r_l} \frac{1}{k_l} (u - \hat{r}_l) du. \quad (46)$$

Then

$$\begin{aligned} \dot{V} &= \frac{dV}{dt} \\ &= \sum_{l \in L} (r_l - \hat{r}_l) \left[ \sum_{s: l \in S} x_s - \sum_{h \in H} \lambda_{l,h} q_h(\beta \mathbf{r}) \right]_{r_l}^+ \\ &\quad + \sum_{s \in S} (x_s - \hat{x}_s) \left[ U'_s(x_s) - \sum_{l: l \in S} r_l \right]_{x_s}^+ \\ &\leq \sum_{l \in L} (r_l - \hat{r}_l) \left[ \sum_{s: l \in S} x_s - \sum_{h \in H} \lambda_{l,h} q_h(\beta \mathbf{r}) \right] \\ &\quad + \sum_{s \in S} (x_s - \hat{x}_s) \left[ U'_s(x_s) - \sum_{l: l \in S} r_l \right] \\ &\leq 0 \text{ because of (44) and (45)} \end{aligned}$$

Further,  $\frac{dV}{dt} = 0$  only when  $r_l = \hat{r}_l, l \in L$  and  $x_s = \hat{x}_s, s \in S$ . We also have that the Lyapunov function  $V(\mathbf{x}, \mathbf{r})$  is radially unbounded.  $V(\hat{\mathbf{x}}, \hat{\mathbf{r}}) = 0$  and  $V(\mathbf{x}, \mathbf{r}) > 0, \forall \mathbf{x} > \hat{\mathbf{x}}, \mathbf{r} > \hat{\mathbf{r}}$ .

Then the globally asymptotic stability comes from the Lyapunov theorem [51]. Thus the dynamic system defined by the primal-dual algorithm (14) converges to the unique optimal solution of the problem  $\mathbf{DP} - \beta$  (13).

#### D. Proof of Theorem 3

Part of the proof hinges on a lemma due to Robbins and Siegmund [52], which is restated as follows.

**Lemma 1.** *Let  $(\Omega, \mathcal{F}, \mathcal{P})$  be a probability space and let  $\mathcal{F}_0 \subset \mathcal{F}_1 \subset \dots$  be a sequence of sub  $\sigma$ -fields of  $\mathcal{F}$ . Let  $u_m$  and  $v_m, m = 0, 1, 2, \dots$ , be non-negative  $\mathcal{F}_m$ -measurable random variables. Assume that*

$$E[v_{m+1}|\mathcal{F}_m] \leq v_m - u_m$$

hold with probability 1. Then, with probability 1, the sequence  $\{v_m\}$  converges to a non-negative random variable and  $\sum_{m=0}^{\infty} u_m < \infty$ .

Now we begin the proof of theorem 3.

Before the further illustration, we need some notation. The vector  $\mathbf{x}$  and the vector  $\mathbf{r}$  are updated at time  $t_m, m = 1, 2, \dots$  with  $t_0 = 0$ . Define  $T_m = t_{m+1} - t_m$ , and the ‘‘period  $m$ ’’ as the time between  $t_m$  and  $t_{m+1}, m = 0, 1, 2, \dots$ .  $\mathbf{x}(t), \mathbf{r}(t)$  remain the same in period  $m$ . Let  $\mathbf{x}(m), \mathbf{r}(m)$  be the value of  $\mathbf{x}(t), \mathbf{r}(t)$  for all  $t \in [t_m, t_{m+1})$ . To begin with, we assume  $\mathbf{x}(0) = \mathbf{0}$  and  $\mathbf{r}(0) = \mathbf{0}$  for simplicity. Let  $\theta_l(m) = \sum_{h \in H} \lambda_{l,h} q_h(\beta \mathbf{r}(m))$  denote the link rate for link  $l$  in period  $m$ . Then let  $\bar{\theta}_l(m)$  be the average link rate measured by link  $l$  within period  $m$ .

Let  $\mathbf{y}^0(m)$  be the state of the Markov chain at the beginning of period  $m$ . Define the random vector  $U(m) = (\bar{\theta}(m-1), \mathbf{x}(m), \mathbf{r}(m), \mathbf{y}^0(m))$  for  $m \geq 1$  and  $U(0) = (\mathbf{x}(0), \mathbf{r}(0), \mathbf{y}^0(0))$ . For  $m \geq 1$ , let  $\mathcal{F}_m$  be the  $\sigma$ -field generated by  $U(0), U(1), \dots, U(m)$ , denoted by

$$\mathcal{F}_m = \sigma(U(0), U(1), \dots, U(m)). \quad (47)$$

Given  $\mathbf{x}(m), \mathbf{r}(m)$  at the beginning of period  $m$ . Let the vector  $\mathbf{f}(m)$  be the gradient vector of  $L_\beta(\mathbf{x}, \mathbf{r})$  with respect to  $\mathbf{x}$ , and the vector  $\mathbf{g}(m)$  be the gradient vector of  $L_\beta(\mathbf{x}, \mathbf{r})$  with respect to  $\mathbf{r}$ . Then we have

$$\begin{cases} f_s(m) = U'_s(x_s(m)) - \sum_{l:l \in S} r_l(m), \quad \forall s \in S \\ g_l(m) = \theta_l(m) - \sum_{s:l \in S} x_s(m), \quad \forall l \in L \end{cases}, \quad (48)$$

However, in stochastic primal-dual algorithm (15), we only have an estimation of  $g_l(m)$  for all  $l \in L$ , denoted by

$$\bar{g}_l(m) = \bar{\theta}_l(m) - \sum_{s:l \in S} x_s(m), \quad \forall l \in L \quad (49)$$

Then  $\forall l \in L, \bar{g}_l(m)$  can be decomposed into three parts:  $\bar{g}_l(m) = g_l(m) + (E[\bar{g}_l(m)|\mathcal{F}_m] - g_l(m)) + (\bar{g}_l(m) - E[\bar{g}_l(m)|\mathcal{F}_m])$ .

The first part is the exact gradient  $g_l(m)$ . The second part is the biased estimation error of  $g_l(m)$ , denoted by

$$B_l(m) \triangleq E[\bar{g}_l(m)|\mathcal{F}_m] - g_l(m) = E[\bar{\theta}_l(m)|\mathcal{F}_m] - \theta_l(m). \quad (50)$$

The third part is a zero-mean martingale difference noise, denoted by

$$\eta_l(m) \triangleq \bar{g}_l(m) - E[\bar{g}_l(m)|\mathcal{F}_m] = \bar{\theta}_l(m) - E[\bar{\theta}_l(m)|\mathcal{F}_m]. \quad (51)$$

Therefore,

$$\bar{g}_l(m) = g_l(m) + B_l(m) + \eta_l(m), \quad \forall l \in L \quad (52)$$

Recall that  $(\hat{\mathbf{x}}, \hat{\mathbf{r}})$  is the optimal solution to the problem  $\mathbf{DP} - \beta$  (13). Thus  $(\hat{\mathbf{x}}, \hat{\mathbf{r}})$  is a saddle point for  $L_\beta(\mathbf{x}, \mathbf{r})$ , it follows that

$$L_\beta(\mathbf{x}, \hat{\mathbf{r}}) \leq L_\beta(\hat{\mathbf{x}}, \hat{\mathbf{r}}) \leq L_\beta(\hat{\mathbf{x}}, \mathbf{r}). \quad (53)$$

By using  $\|\cdot\|$  to denote the Euclidean norm, we define the function  $V(\cdot, \cdot)$  as follows:

$$V(\mathbf{x}, \mathbf{r}) \triangleq \|\mathbf{x} - \hat{\mathbf{x}}\|^2 + \|\mathbf{r} - \hat{\mathbf{r}}\|^2. \quad (54)$$

Since

$$\begin{aligned} x_s(m+1) &= [x_s(m) + \epsilon \cdot f_s(m)]_+, \quad \forall s \in S \\ r_l(m+1) &= [r_l(m) - \epsilon \cdot \bar{g}_l(m)]_+, \quad \forall l \in L \end{aligned}$$

by using the fact that the projection  $[\cdot]_+$  is non-expansive [43], we have

$$\begin{aligned} \|\mathbf{x}(m+1) - \hat{\mathbf{x}}\|^2 &\leq \|\mathbf{x}(m) + \epsilon \cdot \mathbf{f}(m) - \hat{\mathbf{x}}\|^2 \\ &= \|\mathbf{x}(m) - \hat{\mathbf{x}}\|^2 + 2\epsilon \cdot [\mathbf{x}(m) - \hat{\mathbf{x}}]^T \mathbf{f}(m) \\ &\quad + \epsilon^2(m) \|\mathbf{f}(m)\|^2. \end{aligned}$$

Similarly, with (52), we have

$$\begin{aligned} \|\mathbf{r}(m+1) - \hat{\mathbf{r}}\|^2 &\leq \|\mathbf{r}(m) - \epsilon \cdot \bar{\mathbf{g}}(m) - \hat{\mathbf{r}}\|^2 \\ &= \|\mathbf{r}(m) - \hat{\mathbf{r}}\|^2 - 2\epsilon \cdot [\mathbf{r}(m) - \hat{\mathbf{r}}]^T \bar{\mathbf{g}}(m) \\ &\quad + \epsilon^2(m) \|\bar{\mathbf{g}}(m)\|^2 \\ &= \|\mathbf{r}(m) - \hat{\mathbf{r}}\|^2 - 2\epsilon \cdot [\mathbf{r}(m) - \hat{\mathbf{r}}]^T [\mathbf{g}(m) \\ &\quad + \mathbf{B}(m) + \boldsymbol{\eta}(m)] + \epsilon^2(m) \|\bar{\mathbf{g}}(m)\|^2. \end{aligned}$$

By assumption,  $U'_s(\cdot), x_s(m)$  and  $r_l(m)$  are bounded for all  $s, l, m$ , thus with (48) and (49), we know that both  $\|\mathbf{f}(m)\|^2$  and  $\|\bar{\mathbf{g}}(m)\|^2$  are bounded, we can write that  $\|\mathbf{f}(m)\|^2 \leq C_1$  and  $\|\bar{\mathbf{g}}(m)\|^2 \leq C_2$ , where  $C_1$  and  $C_2$  are positive constants. Using this and the above inequalities, we have that

$$\begin{aligned} &V(\mathbf{x}(m+1), \mathbf{r}(m+1)) \\ &= \|\mathbf{x}(m+1) - \hat{\mathbf{x}}\|^2 + \|\mathbf{r}(m+1) - \hat{\mathbf{r}}\|^2 \\ &\leq V(\mathbf{x}(m), \mathbf{r}(m)) + 2\epsilon \cdot [(\mathbf{x}(m) - \hat{\mathbf{x}})^T \mathbf{f}(m) \\ &\quad - (\mathbf{r}(m) - \hat{\mathbf{r}})^T \mathbf{g}(m)] - 2\epsilon \cdot [\mathbf{r}(m) - \hat{\mathbf{r}}]^T [\mathbf{B}(m) + \boldsymbol{\eta}(m)] \\ &\quad + \epsilon^2(m) \cdot (C_1 + C_2). \end{aligned} \quad (55)$$

Since  $L_\beta(\mathbf{x}, \mathbf{r})$  is concave in  $\mathbf{x}$  and convex in  $\mathbf{r}$ ,  $\mathbf{f}(m)$  and  $\mathbf{g}(m)$  are the gradient vectors of  $L_\beta(\mathbf{x}, \mathbf{r})$  with respect to  $\mathbf{x}$  and  $\mathbf{r}$  respectively, it follows that

$$L_\beta(\mathbf{x}(m), \mathbf{r}(m)) - L_\beta(\hat{\mathbf{x}}, \mathbf{r}(m)) \geq (\mathbf{x}(m) - \hat{\mathbf{x}})^T \mathbf{f}(m), \quad (56)$$

$$L_\beta(\mathbf{x}(m), \hat{\mathbf{r}}) - L_\beta(\mathbf{x}(m), \mathbf{r}(m)) \geq -(\mathbf{r}(m) - \hat{\mathbf{r}})^T \mathbf{g}(m). \quad (57)$$

By the summation of (56) and (57), we have

$$\begin{aligned} & (\mathbf{x}(m) - \hat{\mathbf{x}})^T \mathbf{f}(m) - (\mathbf{r}(m) - \hat{\mathbf{r}})^T \mathbf{g}(m) \\ & \leq L_\beta(\mathbf{x}(m), \hat{\mathbf{r}}) - L_\beta(\hat{\mathbf{x}}, \mathbf{r}(m)). \end{aligned} \quad (58)$$

Combining with (55) yields that

$$\begin{aligned} & V(\mathbf{x}(m+1), \mathbf{r}(m+1)) \\ & \leq V(\mathbf{x}(m), \mathbf{r}(m)) + 2\epsilon \cdot [L_\beta(\mathbf{x}(m), \hat{\mathbf{r}}) - L_\beta(\hat{\mathbf{x}}, \mathbf{r}(m))] \\ & + 2\epsilon \cdot [\hat{\mathbf{r}} - \mathbf{r}(m)]^T [\mathbf{B}(m) + \boldsymbol{\eta}(m)] + \epsilon^2(m) \cdot (C_1 + C_2). \end{aligned} \quad (59)$$

Further,

$$\begin{aligned} & E[V(\mathbf{x}(m+1), \mathbf{r}(m+1)) | \mathcal{F}_m] \\ & \leq V(\mathbf{x}(m), \mathbf{r}(m)) + 2\epsilon \cdot [L_\beta(\mathbf{x}(m), \hat{\mathbf{r}}) - L_\beta(\hat{\mathbf{x}}, \mathbf{r}(m))] \\ & + 2\epsilon \cdot [\hat{\mathbf{r}} - \mathbf{r}(m)]^T [\mathbf{B}(m)] + \epsilon^2(m) \cdot (C_1 + C_2) \quad (60) \\ & \leq V(\mathbf{x}(m), \mathbf{r}(m)) + 2\epsilon \cdot [L_\beta(\mathbf{x}(m), \hat{\mathbf{r}}) - L_\beta(\hat{\mathbf{x}}, \mathbf{r}(m))] \\ & + 2\epsilon \cdot \frac{C_3}{T_0} + \epsilon^2(m) \cdot (C_1 + C_2), \end{aligned} \quad (61)$$

where (61) utilizes the result in the following lemma. The proof of it is given at Appendix-E.

**Lemma 2.**

$$|[\hat{\mathbf{r}} - \mathbf{r}(m)]^T \mathbf{B}(m)| \leq \frac{C_3}{T_0}, \quad \forall m \quad (62)$$

Now we define the set

$$\begin{aligned} H_b = \{(\mathbf{x}, \mathbf{r}) : 0 \leq L_\beta(\hat{\mathbf{x}}, \mathbf{r}) - L_\beta(\mathbf{x}, \hat{\mathbf{r}}) \\ < \frac{1}{b} + \frac{C_3}{T_0} + \epsilon \frac{(C_1 + C_2)}{2}\}, \end{aligned} \quad (63)$$

where  $b$  is a positive constant.

We also define the sequence  $(\mathbf{x}'(m), \mathbf{r}'(m))$  as follows:

$$\begin{aligned} & (\mathbf{x}'(m+1), \mathbf{r}'(m+1)) \quad (64) \\ & = \begin{cases} (\mathbf{x}(m+1), \mathbf{r}(m+1)) & \text{if } (\mathbf{x}'(m), \mathbf{r}'(m)) \notin H_b \\ (\hat{\mathbf{x}}, \hat{\mathbf{r}}) & \text{if } (\mathbf{x}'(m), \mathbf{r}'(m)) \in H_b \end{cases} \end{aligned} \quad (65)$$

Thus the process  $\{(\mathbf{x}'(m), \mathbf{r}'(m))\}$  is identical to the process  $\{(\mathbf{x}(m), \mathbf{r}(m))\}$ , until  $\{(\mathbf{x}(m), \mathbf{r}(m))\}$  enters the set  $H_b$ .

Given  $m$ , we discuss two cases.

**Case 1:**  $(\mathbf{x}'(m), \mathbf{r}'(m)) \in H_b$ .

Since  $(\mathbf{x}'(m), \mathbf{r}'(m)) \in H_b$  and  $(\mathbf{x}'(m+1), \mathbf{r}'(m+1)) = (\hat{\mathbf{x}}, \hat{\mathbf{r}})$ , we have  $V(\mathbf{x}'(m+1), \mathbf{r}'(m+1)) = 0$  and  $V(\mathbf{x}'(m), \mathbf{r}'(m)) \geq 0$ , yielding

$$E[V(\mathbf{x}'(m+1), \mathbf{r}'(m+1)) | \mathcal{F}_m] \leq V(\mathbf{x}'(m), \mathbf{r}'(m)). \quad (66)$$

**Case 2:**  $(\mathbf{x}'(m), \mathbf{r}'(m)) \notin H_b$ .

Then we have  $(\mathbf{x}'(m), \mathbf{r}'(m)) = (\mathbf{x}(m), \mathbf{r}(m))$  and  $(\mathbf{x}'(m+1), \mathbf{r}'(m+1)) = (\mathbf{x}(m+1), \mathbf{r}(m+1))$ . Using (61), we have

$$\begin{aligned} & E[V(\mathbf{x}'(m+1), \mathbf{r}'(m+1)) | \mathcal{F}_m] \\ & \leq V(\mathbf{x}'(m), \mathbf{r}'(m)) + 2\epsilon [L_\beta(\mathbf{x}'(m), \hat{\mathbf{r}}) - L_\beta(\hat{\mathbf{x}}, \mathbf{r}'(m))] \\ & + 2\epsilon \cdot \frac{C_3}{T_0} + \epsilon^2 \cdot (C_1 + C_2). \end{aligned} \quad (67)$$

Observe that when  $(\mathbf{x}'(m), \mathbf{r}'(m)) \notin H_b$ ,

$$L_\beta(\hat{\mathbf{x}}, \mathbf{r}'(m)) - L_\beta(\mathbf{x}'(m), \hat{\mathbf{r}}) \geq \frac{1}{b} + \frac{C_3}{T_0} + \epsilon \frac{(C_1 + C_2)}{2}. \quad (68)$$

Therefore, by combining (67) and (68), we obtain that

$$E[V(\mathbf{x}'(m+1), \mathbf{r}'(m+1)) | \mathcal{F}_m] \leq V(\mathbf{x}'(m), \mathbf{r}'(m)) - \frac{2\epsilon}{b}. \quad (69)$$

Then from (66) and (69), we can write

$$E[V(\mathbf{x}'(m+1), \mathbf{r}'(m+1)) | \mathcal{F}_m] \leq V(\mathbf{x}'(m), \mathbf{r}'(m)) - \Delta(m), \quad (70)$$

where

$$\Delta(m) = \begin{cases} 0 & \text{if } (\mathbf{x}'(m), \mathbf{r}'(m)) \in H_b \\ \frac{2\epsilon}{b} & \text{if } (\mathbf{x}'(m), \mathbf{r}'(m)) \notin H_b \end{cases} \quad (71)$$

Observe that (70) satisfies the condition of Lemma 1. Therefore, it follows that with probability 1,

$$\sum_{m=0}^{\infty} \Delta(m) < \infty. \quad (72)$$

However, this is possible only if  $\Delta(m) = 0$  for all sufficiently large  $m$ . Therefore, for any given  $b > 0$ , with probability 1, we have  $(\mathbf{x}'(m), \mathbf{r}'(m)) \in H_b$  for all sufficiently large  $m$ . This also means that for any given  $b > 0$ , with probability 1,  $(\mathbf{x}(m), \mathbf{r}(m)) \in H_b$  for all sufficiently large  $m$ . By letting  $b \rightarrow \infty$ , we have that with probability 1, and for all sufficiently large  $m$ ,  $(\mathbf{x}(m), \mathbf{r}(m))$  belongs to the set

$$\left\{ (\mathbf{x}, \mathbf{r}) : 0 \leq L_\beta(\hat{\mathbf{x}}, \mathbf{r}) - L_\beta(\mathbf{x}, \hat{\mathbf{r}}) \leq \frac{C_3}{T_0} + \epsilon \frac{(C_1 + C_2)}{2} \right\}.$$

It follows that with probability 1, for all sufficiently large  $m$ ,

$$0 \leq L_\beta(\hat{\mathbf{x}}, \mathbf{r}(m)) - L_\beta(\mathbf{x}(m), \hat{\mathbf{r}}) \leq \frac{C_3}{T_0} + \epsilon \frac{(C_1 + C_2)}{2}.$$

Then we have

$$L_\beta(\mathbf{x}(m), \mathbf{r}(m)) \leq L_\beta(\hat{\mathbf{x}}, \mathbf{r}(m)) \quad (73)$$

$$\leq L_\beta(\mathbf{x}(m), \hat{\mathbf{r}}) + \frac{C_3}{T_0} + \epsilon \frac{(C_1 + C_2)}{2} \quad (74)$$

$$\leq L_\beta(\hat{\mathbf{x}}, \hat{\mathbf{r}}) + \frac{C_3}{T_0} + \epsilon \frac{(C_1 + C_2)}{2} \quad (75)$$

and

$$L_\beta(\mathbf{x}(m), \mathbf{r}(m)) \geq L_\beta(\mathbf{x}(m), \hat{\mathbf{r}}) \quad (76)$$

$$\geq L_\beta(\hat{\mathbf{x}}, \mathbf{r}(m)) - \left( \frac{C_3}{T_0} + \epsilon \frac{(C_1 + C_2)}{2} \right) \quad (77)$$

$$\geq L_\beta(\hat{\mathbf{x}}, \hat{\mathbf{r}}) - \left( \frac{C_3}{T_0} + \epsilon \frac{(C_1 + C_2)}{2} \right) \quad (78)$$

Therefore, with probability 1, for all sufficiently large  $m$ ,

$$|L_\beta(\mathbf{x}(m), \mathbf{r}(m)) - L_\beta(\hat{\mathbf{x}}, \hat{\mathbf{r}})| \leq \frac{C_3}{T_0} + \epsilon \frac{(C_1 + C_2)}{2}. \quad (79)$$

Thus with probability 1,  $\{(\mathbf{x}(m), \mathbf{r}(m))\}$  converges to the neighborhood of  $(\hat{\mathbf{x}}, \hat{\mathbf{r}})$ :

$$\left\{ (\mathbf{x}, \mathbf{r}) : |L_\beta(\mathbf{x}, \mathbf{r}) - L_\beta(\hat{\mathbf{x}}, \hat{\mathbf{r}})| \leq \frac{C_3}{T_0} + \epsilon \frac{(C_1 + C_2)}{2} \right\}. \quad (80)$$

This concludes the proof.

### E. Proof of Lemma 2

In the following, we consider the period  $m$ , *i.e.*, from  $t_m$  to  $t_{m+1}$ . At time  $t_m$  with vector  $\mathbf{r}(m)$ , denote the corresponding Markov chain by  $Y(t)$ .  $Y(t)$  is a continuous time Markov chain.

Each state  $\mathbf{y}$  is a  $|L|$ -dimensional vector, with  $l$ -th element  $y_l = \lambda_{l,y}$ , where  $\lambda_{l,y} \in \{0, 1, \dots, \lambda_l\}$  denote the capacity of link  $l$  at state  $\mathbf{y}$ ,  $\forall l \in L$ . Let  $\lambda_{\max} \triangleq \max_{l \in L} \lambda_l$  and  $K \triangleq \lambda_{\max} + 1$ . Thus the number of states is  $|Y| \leq K^{|L|}$ .

By (10), the stationary distribution of state  $\mathbf{y}$  is

$$\begin{aligned} \pi_{\mathbf{y}}(\mathbf{r}(m)) &= q_{\mathbf{y}}(\beta \mathbf{r}) = \frac{\exp(\beta \sum_{l \in L} \lambda_{l,y} r_l)}{\sum_{\mathbf{y}} \exp(\beta \sum_{l \in L} \lambda_{l,y} r_l)} \\ &= \frac{\exp(\beta \sum_{l \in L} \lambda_{l,y} r_l)}{C(\mathbf{r}(m))}, \forall \mathbf{y}, \end{aligned} \quad (81)$$

where  $C(\mathbf{r}(m)) = \sum_{\mathbf{y}} \exp(\beta \sum_{l \in L} \lambda_{l,y} r_l)$ .

Since  $\mathbf{r}(m) \geq \mathbf{0}$ ,  $C(\mathbf{r}(m)) \leq \sum_{\mathbf{y}} \exp(\beta \lambda_{\max} \mathbf{1}^T \mathbf{r}(m)) \leq$

$K^{|L|} \exp(\beta \lambda_{\max} \mathbf{1}^T \mathbf{r}(m))$ .

Thus the minimal probability in the stationary distribution

$$\begin{aligned} \pi_{\min}(\mathbf{r}(m)) &\triangleq \min_{\mathbf{y}} \pi_{\mathbf{y}}(\mathbf{r}(m)) \geq \frac{1}{C(\mathbf{r}(m))} \\ &= \exp(-|L| \cdot \log |K| - \beta \lambda_{\max} \mathbf{1}^T \mathbf{r}(m)). \end{aligned} \quad (82)$$

Since  $r_{\max} = \max_{l,m} r_l(m) < \infty$ , we have

$$\begin{aligned} \pi_{\min}(\mathbf{r}(m)) &\geq \exp(-|L| \cdot \log |K| - \beta \lambda_{\max} |L| r_{\max}) \\ &= \exp(-|L| \cdot (\log |K| + \beta \lambda_{\max} r_{\max})). \end{aligned} \quad (83)$$

To utilize the existing bounds on convergence to the stationary distribution of discrete-time Markov chain, we uniformize the continuous-time Markov chain  $Y(t)$ . Uniformization [50] plays the role of bridge between discrete-time Markov chain and continuous-time Markov chain.

Let the transition rate matrix of  $Y(t)$  is denoted by  $Q = \{Q(\mathbf{y}, \mathbf{y}')\}$ . Construct a discrete-time Markov chain  $Z(n)$  with its probability transition matrix  $P = I + Q/v_m$ , where  $I$  is the identity matrix. Then consider a system that successive

states visited form a Markov chain  $Z(n)$  and the times at which the system changes its state form a Poisson process  $N(t)$ . Here  $N(t)$  is an independent Poisson process with rate  $v_m$ . Then the state of this system at time  $t$  is denoted by  $Z(N(t))$ , which is called a *subordinated Markov chain*.

Let

$$v_m = |L| \cdot \exp(\beta \lambda_{\max} r_{\max}). \quad (84)$$

Since  $\forall \mathbf{y}, \mathbf{y}'$ ,  $Q(\mathbf{y}, \mathbf{y}') \leq \exp(\beta \lambda_{\max} r_l(m)) \leq \exp(\beta \lambda_{\max} r_{\max})$ , and  $\mathbf{y}$  can at most transit to  $|L|$  other states, thus  $\sum_{\mathbf{y} \neq \mathbf{y}'} Q(\mathbf{y}, \mathbf{y}') \leq |L| \cdot \exp(\beta \lambda_{\max} r_{\max}) = v_m$ . Then by uniformization theorem [50],  $Y(t)$  and  $Z(N(t))$  has the same distribution, denoted by  $Y(t) \stackrel{d}{=} Z(N(t))$ .

Now let the vector  $\omega_m(t) = \{\omega_m(t, \mathbf{y})\}$  be the probabilities of all states at time  $t_m + t$  ( $0 \leq t \leq T_0$ ), given that the initial state at time  $t_m$  is  $\mathbf{y}^0(m)$  and that the link prices during time interval  $[t_m, t_{m+1})$  are  $\mathbf{r}(m)$ . Let  $\mathbf{y}(t_m + t)$  be the state at time  $t_m + t$ , then

$$\begin{aligned} &E[\bar{\theta}_l(m) | \mathcal{F}_m] \\ &= E\left[ \frac{\int_0^{T_0} (1 \cdot I(y_l(t_m + t) = 1) + \dots + \lambda_l \cdot I(y_l(t_m + t) = \lambda_l)) dt}{T_0} \right] \\ &= \frac{\int_0^{T_0} (1 \cdot P(y_l(t_m + t) = 1) + \dots + \lambda_l \cdot P(y_l(t_m + t) = \lambda_l)) dt}{T_0} \\ &= \int_0^{T_0} E[y_l(t_m + t) | \mathcal{F}_m] dt / T_0 \\ &= \int_0^{T_0} \sum_{\mathbf{y}'} \lambda_{l,y'} \cdot \omega_m(t, \mathbf{y}') dt / T_0 \\ &= \sum_{\mathbf{y}'} \lambda_{l,y'} \cdot \int_0^{T_0} \omega_m(t, \mathbf{y}') dt / T_0 \\ &= \sum_{\mathbf{y}'} \lambda_{l,y'} \cdot \bar{\omega}_m(\mathbf{y}'), \end{aligned} \quad (85)$$

where  $\bar{\omega}_m(\mathbf{y}') = \int_0^{T_0} \omega_m(t, \mathbf{y}') dt / T_0$  is the time-averaged probability of state  $\mathbf{y}'$  in the interval.

Since the initial distribution is concentrated at a single definite starting state  $\mathbf{y}^0(m)$ , we denote this distribution by  $\delta_{\mathbf{y}^0}$ . We let  $\pi_{\mathbf{y}^0}(\mathbf{r}(m))$  be the probability of  $\mathbf{y}^0(m)$  in the stationary distribution of  $Y(t)$ . Let  $\pi(\mathbf{r}(m)) \triangleq \{\pi_{\mathbf{y}}(\mathbf{r}(m))\}$  be the stationary distribution of  $Y(t)$ , then by uniformization theorem [50],  $\pi(\mathbf{r}(m))$  is also the stationary distribution of  $Z(n)$ .

We use  $\|\cdot\|_{TV}$  to denote the total variation distance between two distributions [49], which satisfies triangle inequality. We use  $\rho_2$  to denote the second largest eigenvalue of transition matrix  $P$ . Thus for reversible discrete-time Markov chain  $Z(n)$  with transition matrix  $P$ , and for any  $n \geq 0$ , we have the following inequality [49]:

$$\|\delta_{\mathbf{y}^0} P^n - \pi(\mathbf{r}(m))\|_{TV} \leq \frac{1}{2} \sqrt{\frac{1 - \pi_{\mathbf{y}^0}(\mathbf{r}(m))}{\pi_{\mathbf{y}^0}(\mathbf{r}(m))}} \cdot \rho_2^n$$

Therefore,

$$\begin{aligned}
& \|\omega_m(t) - \pi(\mathbf{r}(m))\|_{TV} \\
&= \left\| \sum_{n=0}^{\infty} \frac{(v_m t)^n}{n!} \exp(-v_m t) \delta_{\mathbf{y}^0} P^n - \pi(\mathbf{r}(m)) \right\|_{TV} \\
&\leq \sum_{n=0}^{\infty} \frac{(v_m t)^n}{n!} \exp(-v_m t) \|\delta_{\mathbf{y}^0} P^n - \pi(\mathbf{r}(m))\|_{TV} \\
&\leq \frac{1}{2} \sqrt{\frac{1 - \pi_{\mathbf{y}^0}(\mathbf{r}(m))}{\pi_{\mathbf{y}^0}(\mathbf{r}(m))}} \cdot \sum_{n=0}^{\infty} \frac{(v_m t \rho_2)^n}{n!} \exp(-v_m t) \\
&= \frac{1}{2} \sqrt{\frac{1 - \pi_{\mathbf{y}^0}(\mathbf{r}(m))}{\pi_{\mathbf{y}^0}(\mathbf{r}(m))}} \cdot \exp(-v_m(1 - \rho_2)t) \\
&\leq \frac{1}{2} \sqrt{\frac{1}{\pi_{\min}(\mathbf{r}(m))}} \cdot \exp(-v_m(1 - \rho_2)t)
\end{aligned}$$

Further,

$$\begin{aligned}
& \|\bar{\omega}_m - \pi(\mathbf{r}(m))\|_{TV} \tag{86} \\
&= \left\| \int_0^{T_0} [\omega_m(t) - \pi(\mathbf{r}(m))] dt / T_0 \right\|_{TV} \\
&\leq \int_0^{T_0} \|\omega_m(t) - \pi(\mathbf{r}(m))\|_{TV} dt / T_0 \\
&\leq \frac{1}{2} \sqrt{\frac{1}{\pi_{\min}(\mathbf{r}(m))}} \frac{1}{v_m(1 - \rho_2)T_0} \tag{87}
\end{aligned}$$

Now we bound  $\rho_2$  by Cheeger's inequality [49]

$$\rho_2 \leq 1 - \phi^2/2,$$

where  $\phi$  is the ‘‘Conductance’’ of  $P$ , defined as

$$\phi \triangleq \min_{N \subset \Omega, \pi(N) \in (0, 1/2]} \frac{F(N, N^c)}{\pi_N(\mathbf{r}(m))}.$$

Here  $\Omega$  is the state space,  $\pi_N(\mathbf{r}(m)) = \sum_{\mathbf{y} \in N} \pi_{\mathbf{y}}(\mathbf{r}(m))$  and  $F(N, N^c) = \sum_{\mathbf{y} \in N, \mathbf{y}' \in N^c} \pi_{\mathbf{y}}(\mathbf{r}(m)) P(\mathbf{y}, \mathbf{y}')$ .

Thus

$$\begin{aligned}
\phi &\geq \min_{N \subset \Omega, \pi(N) \in (0, 1/2]} F(N, N^c) \\
&\geq \min_{\mathbf{y} \neq \mathbf{y}', P(\mathbf{y}, \mathbf{y}') > 0} F(\mathbf{y}, \mathbf{y}') \\
&= \min_{\mathbf{y} \neq \mathbf{y}', P(\mathbf{y}, \mathbf{y}') > 0} \pi_{\mathbf{y}}(\mathbf{r}(m)) P(\mathbf{y}, \mathbf{y}') \\
&\geq \min_{\mathbf{y}} \pi_{\mathbf{y}}(\mathbf{r}(m)) / v_m \\
&= \pi_{\min}(\mathbf{r}(m)) / v_m.
\end{aligned}$$

Then

$$\frac{1}{1 - \rho_2} \leq \frac{2}{\phi^2} = 2 \cdot v_m^2 [\pi_{\min}(\mathbf{r}(m))]^{-2}. \tag{88}$$

Combing (88), (83), (84) with (87), it follows that

$$\begin{aligned}
& \|\bar{\omega}_m - \pi(\mathbf{r}(m))\|_{TV} \\
&\leq \frac{v_m}{T_0} [\pi_{\min}(\mathbf{r}(m))]^{-5/2} \\
&= (|L|/T_0) \cdot \exp[(5/2|L| + 1)\beta\lambda_{\max}r_{\max} + 5/2|L| \log |K|] \\
&= (|L| \cdot \tau) / T_0,
\end{aligned}$$

where  $\tau = \exp[(5/2|L| + 1)\beta\lambda_{\max}r_{\max} + 5/2|L| \log |K|]$ .

Then by (50) and (85), we have

$$\begin{aligned}
|B_l(m)| &= |E[\bar{\theta}_l(m)|\mathcal{F}_m] - \theta_l(m)| \\
&= \left| \sum_{\mathbf{y}'} \lambda_{l, \mathbf{y}'} \cdot \bar{\omega}_m(\mathbf{y}') - \sum_{\mathbf{y}'} \lambda_{l, \mathbf{y}'} \cdot \pi_{\mathbf{y}'}(\mathbf{r}(m)) \right| \\
&\leq \lambda_{\max} \cdot 2 \|\bar{\omega}_m - \pi(\mathbf{r}(m))\|_{TV} \\
&\leq (2|L|\lambda_{\max} \cdot \tau) / T_0, \forall l \in L.
\end{aligned}$$

Since  $\forall l \in L$ ,  $\hat{r}_l$  is bounded and  $\hat{r}_l < \bar{r}$  for some  $\bar{r} > 0$ , then we have

$$|[\hat{r}_l - r_l(m)]| \leq \bar{r} + r_{\max}, \forall l \in L.$$

Therefore

$$\begin{aligned}
& [\hat{\mathbf{r}} - \mathbf{r}(m)]^T \mathbf{B}(m) \\
&\leq |L| \cdot \frac{2|L|\lambda_{\max}\tau}{T_0} \cdot (\bar{r} + r_{\max}) \\
&= \frac{C_3}{T_0}.
\end{aligned}$$

where  $C_3 = 2|L|^2\lambda_{\max}\tau(\bar{r} + r_{\max})$  is a positive constant. This concludes the proof.

## REFERENCES

- [1] A. Avestimehr, S. Diggavi, and D. Tse, ‘‘A deterministic approach to wireless relay networks,’’ in *Proceedings of Allerton 2007*.
- [2] —, ‘‘Wireless network information flow: a deterministic approach,’’ to appear in *IEEE Transactions on Information Theory*, 2011, available at <http://arxiv.org/abs/0906.5394>.
- [3] F. Kelly, A. Maulloo, and D. Tan, ‘‘Rate control for communication networks: shadow prices, proportional fairness and stability,’’ *Journal of the Operational Research society*, vol. 49, no. 3, pp. 237–252, 1998.
- [4] M. Chiang, S. Low, A. Calderbank, and J. Doyle, ‘‘Layering as optimization decomposition: A mathematical theory of network architectures,’’ *Proceedings of the IEEE*, vol. 95, no. 1, pp. 255–312, 2007.
- [5] X. Lin, N. Shroff, and R. Srikant, ‘‘A tutorial on cross-layer optimization in wireless networks,’’ *IEEE Journal on Selected Areas in Communications*, vol. 24, no. 8, pp. 1452–1463, 2006.
- [6] D. Tse and S. Hanly, ‘‘Multi-access fading channels: part I: polymatroid structure, optimal resource allocation and throughput capacities,’’ *IEEE Transactions on Information Theory*, vol. 44, no. 7, pp. 2796–2815, 1998.
- [7] L. Li and A. Goldsmith, ‘‘Capacity and optimal resource allocation for fading broadcast channels. I. Ergodic capacity,’’ *IEEE Transactions on Information Theory*, vol. 47, no. 3, pp. 1083–1102, 2001.
- [8] J. Liu, Y. Thomas Hou, and H. Sherali, ‘‘Cross-Layer optimization for MIMO-based mesh networks with dirty paper coding,’’ in *Proceedings of IEEE ICC 2008*.
- [9] T. Cover and J. Thomas, *Elements of Information Theory*. New York: Wiley, 2006.
- [10] D. Gesbert, S. Kiani, and A. Gjedemsi, ‘‘Adaptation, coordination, and distributed resource allocation in interference-limited wireless networks,’’ *Proceedings of the IEEE*, vol. 95, no. 12, pp. 2393–2409, 2007.
- [11] C. Tan, M. Chiang, and R. Srikant, ‘‘Fast algorithms and performance bounds for sum rate maximization in wireless networks,’’ in *Proceedings of IEEE INFOCOM 2009*.
- [12] V. Cadambe and S. Jafar, ‘‘Interference Alignment and Degrees of Freedom of the  $K$ -User Interference Channel,’’ *IEEE Transactions on Information Theory*, vol. 54, no. 8, pp. 3425–3441, 2008.
- [13] L. Tassiulas and A. Ephremides, ‘‘Stability properties of constrained queueing systems and scheduling policies for maximum throughput in multihop radio networks,’’ *IEEE Transactions on Automatic Control*, vol. 37, no. 12, pp. 1936–1948, 1992.
- [14] X. Lin and N. Shroff, ‘‘The impact of imperfect scheduling on cross-layer congestion control in wireless networks,’’ *IEEE/ACM Transactions on Networking (TON)*, vol. 14, no. 2, pp. 302–315, 2006.
- [15] G. Sharma, N. Shroff, and R. Mazumdar, ‘‘Joint congestion control and distributed scheduling for throughput guarantees in wireless networks,’’ in *Proceedings of IEEE INFOCOM 2007*.

- [16] P. Chaporkar, K. Kar, X. Luo, and S. Sarkar, "Throughput and fairness guarantees through maximal scheduling in wireless networks," *IEEE Transactions on Information Theory*, vol. 54, no. 2, pp. 572–594, 2008.
- [17] A. Avestimehr, S. Diggavi, and D. Tse, "Wireless network information flow," in *Proceedings of Allerton 2007*.
- [18] M. Chen, S. Liew, Z. Shao, and C. Kai, "Markov Approximation for Combinatorial Network Optimization," in *Proceedings of IEEE INFOCOM 2010*.
- [19] K. Jain, J. Padhye, V. Padmanabhan, and L. Qiu, "Impact of interference on multi-hop wireless network performance," *Wireless Networks*, vol. 11, no. 4, pp. 471–487, 2005.
- [20] L. Jiang and J. Walrand, "A distributed csma algorithm for throughput and utility maximization in wireless networks," in *Proceedings of Allerton 2008*.
- [21] J. Liu, Y. Yi, A. Proutiere, M. Chiang, and H. Poor, "Convergence and Tradeoff of Utility-Optimal CSMA," *submitted for publication*, 2009, available at <http://arxiv.org/abs/0902.1996>.
- [22] Jiang, L. and Walrand, J., "Convergence and stability of a distributed csma algorithm for maximal network throughput," *Technical Report*, 2009, available at <http://www.eecs.berkeley.edu/Pubs/TechRpts/2009/EECS-2009-43.html>.
- [23] Y. Wang, W. Wang, X. Li, and W. Song, "Interference-aware joint routing and TDMA link scheduling for static wireless networks," *IEEE Transactions on Parallel and Distributed Systems*, vol. 19, no. 12, pp. 1709–1726, 2008.
- [24] L. Jiang and J. Walrand, "A distributed CSMA algorithm for throughput and utility maximization in wireless networks," *IEEE/ACM Transactions on Networking*, vol. 18, no. 3, pp. 960–972, 2010.
- [25] A. Eryilmaz, A. Ozdaglar, D. Shah, and E. Modiano, "Distributed cross-layer algorithms for the optimal control of multihop wireless networks," *IEEE/ACM Transactions on Networking*, vol. 18, no. 2, pp. 638–651, 2010.
- [26] R. Etkin, D. Tse, and H. Wang, "Gaussian interference channel capacity to within one bit," *IEEE Transactions on Information Theory*, vol. 54, no. 12, pp. 5534–5562, 2008.
- [27] G. Bresler and D. Tse, "The two-user Gaussian interference channel: a deterministic view," *European Transactions on Telecommunications*, vol. 19, no. 4, pp. 333–354, 2008.
- [28] S. Mohajer, S. Diggavi, C. Fragouli, and D. Tse, "Approximate Capacity of Gaussian Interference-Relay Networks with Weak Cross Links," *submitted to IEEE Transactions on Information Theory*, April 2010, available at <http://arxiv.org/abs/1005.0404>.
- [29] A. Sezgin, A. Avestimehr, M. Khajehnejad, and B. Hassibi, "Divide-and-conquer: Approaching the capacity of the two-pair bidirectional Gaussian relay network," *submitted to IEEE Transactions on Information Theory*, 2010, available at <http://arxiv.org/abs/1001.4271>.
- [30] G. Bresler, A. Parekh, and D. Tse, "The approximate capacity of the many-to-one and one-to-many Gaussian interference channels," *IEEE Transactions on Information Theory*, vol. 56, no. 9, pp. 4566–4592, 2010.
- [31] G. Sharma, R. Mazumdar, and N. Shroff, "On the complexity of scheduling in wireless networks," in *Proceedings of ACM MobiCom 2006*.
- [32] A. Dimakis and J. Walrand, "Sufficient conditions for stability of longest-queue-first scheduling: Second-order properties using fluid limits," *Advances in Applied probability*, vol. 38, no. 2, pp. 505–521, 2006.
- [33] M. Leconte, J. Ni, and R. Srikant, "Improved bounds on the throughput efficiency of greedy maximal scheduling in wireless networks," in *Proceedings of ACM MobiHoc 2009*.
- [34] C. Joo, X. Lin, and N. Shroff, "Understanding the capacity region of the greedy maximal scheduling algorithm in multihop wireless networks," *IEEE/ACM Transactions on Networking*, vol. 17, no. 4, pp. 1132–1145, 2009.
- [35] B. Birand, M. Chudnovsky, B. Ries, P. Seymour, G. Zussman, and Y. Zwols, "Analyzing the performance of greedy maximal scheduling via local pooling and graph theory," in *Proceedings of IEEE INFOCOM 2010*.
- [36] S. Rajagopalan and D. Shah, "Distributed algorithm and reversible network," in *Proceedings of CISS 2008*.
- [37] S. Rajagopalan, D. Shah, and J. Shin, "Network adiabatic theorem: an efficient randomized protocol for contention resolution," in *Proceedings of ACM Sigmetrics 2009*.
- [38] J. Ni, B. Tan, and R. Srikant, "Q-CSMA: Queue-Length Based CSMA/CA Algorithms for Achieving Maximum Throughput and Low Delay in Wireless Networks," in *Proceedings of IEEE INFOCOM Mini-Conference 2010*.
- [39] J. Mo and J. Walrand, "Fair end-to-end window-based congestion control," *IEEE/ACM Transactions on Networking*, vol. 8, no. 5, pp. 556–567, 2000.
- [40] R. Srikant, *The Mathematics of Internet Congestion Control*. Birkhauser, 2004.
- [41] M. Chen, M. Ponec, S. Sengupta, J. Li, and P. Chou, "Utility maximization in peer-to-peer systems," in *Proceedings of ACM Sigmetrics 2008*.
- [42] T. Voice, "Stability of congestion control algorithms with multi-path routing and linear stochastic modelling of congestion control," *Ph.D. dissertation, University of Cambridge, Cambridge, UK*, May 2006.
- [43] S. Boyd and L. Vandenberghe, *Convex Optimization*. Cambridge university press, 2004.
- [44] V. Vazirani, *Approximation Algorithms*. Springer, 2001.
- [45] F. Kelly, *Reversibility and Stochastic Networks*. Wiley, Chichester, 1979.
- [46] L. Jiang, D. Shah, J. Shin, and J. Walrand, "Distributed Random Access Algorithm: Scheduling and Congestion Control," *IEEE Transactions on Information Theory*, vol. 56, no. 12, pp. 6182–6207, 2010.
- [47] H. Kushner and G. Yin, *Stochastic Approximation and Recursive Algorithms and Applications*. Springer Verlag, 2003.
- [48] J. Zhang, D. Zheng, and M. Chiang, "The impact of stochastic noisy feedback on distributed network utility maximization," *IEEE Transactions on Information Theory*, vol. 54, no. 2, pp. 645–665, 2008.
- [49] P. Diaconis and D. Stroock, "Geometric bounds for eigenvalues of Markov chains," *The Annals of Applied Probability*, vol. 1, no. 1, pp. 36–61, 1991.
- [50] M. Kijima, *Markov Processes for Stochastic Modeling*. CRC Press, 1997.
- [51] H. Khalil, *Nonlinear Systems*. Prentice Hall, Englewood Cliffs, NJ, 2001.
- [52] B. Polyak, *Introduction to Optimization*. Optimization Software Inc., 1987.